

SURFICIAL GEOLOGIC MAP OF THE LEVAN AND FAYETTE SEGMENTS OF THE WASATCH FAULT ZONE, JUAB AND SANPETE COUNTIES, UTAH

by

Michael D. Hylland and Michael N. Machette

ISBN 1-55791-791-4



MAP 229
UTAH GEOLOGICAL SURVEY
a division of
Utah Department of Natural Resources
2008

STATE OF UTAH

Jon Huntsman, Jr., Governor

DEPARTMENT OF NATURAL RESOURCES

Michael Styler, Executive Director

UTAH GEOLOGICAL SURVEY

Richard G. Allis, Director

PUBLICATIONS

contact

Natural Resources Map & Bookstore

1594 W. North Temple

Salt Lake City, Utah 84116

telephone: 801-537-3320

toll free: 1-888-UTAH MAP

Web site: mapstore.utah.gov

email: geostore@utah.gov

UTAH GEOLOGICAL SURVEY

contact

1594 W. North Temple, Suite 3110

Salt Lake City, Utah 84116

telephone: 801-537-3300

fax: 801-537-3400

Web site: geology.utah.gov

Although this product represents the work of professional scientists, the Utah Department of Natural Resources, Utah Geological Survey, makes no warranty, expressed or implied, regarding its suitability for any particular use. The Utah Department of Natural Resources, Utah Geological Survey, shall not be liable under any circumstances for any direct, indirect, special, incidental, or consequential damages with respect to claims by users of this product.

The Utah Department of Natural Resources receives federal aid and prohibits discrimination on the basis of race, color, sex, age, national origin, or disability. For information or complaints regarding discrimination, contact Executive Director, Utah Department of Natural Resources, 1594 West North Temple #3710, Box 145610, Salt Lake City, UT 84116-5610 or Equal Employment Opportunity Commission, 1801 L. Street, NW, Washington DC 20507.

SURFICIAL GEOLOGIC MAP OF THE LEVAN AND FAYETTE SEGMENTS OF THE WASATCH FAULT ZONE, JUAB AND SANPETE COUNTIES, UTAH

by
Michael D. Hylland¹ and Michael N. Machette²

ABSTRACT

This map shows the surficial geology along the two southernmost segments of the Wasatch fault zone, the Levan and Fayette segments. Piedmont-slope fan alluvium of middle Pleistocene to late Holocene age dominates Quaternary deposits along the 44-km combined length of the segments. Other regionally important Quaternary deposits along the segments include unconsolidated to semiconsolidated fan alluvium and basin-fill deposits of Quaternary-Tertiary age, and fine-grained lacustrine deposits of late Pleistocene Lake Bonneville. Stream alluvium, landslide deposits, colluvium, and eolian deposits are also present locally.

Combined with scarp-profile analyses and limited paleoseismic data, our mapping helps establish the timing of most recent surface faulting on the Levan and Fayette segments, and allows maximum Holocene and average long-term (geologic) vertical slip rates to be estimated. Stratigraphic data and numerical ages obtained during this study and previously by others indicate the most recent surface-faulting earthquake on the Levan segment occurred shortly after 1000 ± 200 cal yr B.P. Numerical ages previously obtained by others roughly constrain the timing of the penultimate surface-faulting earthquake on the Levan segment to sometime prior to 2800–4300 cal yr B.P., and perhaps prior to 6000–10,600 cal yr B.P. On the Fayette segment, cross-cutting geologic relations and empirical analysis of scarp-profile data indicate the timing of most recent surface faulting is different for the three strands of the segment: early or middle Pleistocene(?) for the northern (N) strand, latest Pleistocene for the southeastern (SE) strand, and Holocene for the southwestern (SW) strand. The timing of earlier surface-faulting earthquakes on the individual strands of the Fayette segment is unknown.

Our preferred maximum Holocene vertical slip rate for the Levan segment, based on limited paleoseismic data, is 0.3 ± 0.1 mm/yr. Estimated middle to late Quaternary vertical slip rates, based on net geomorphic surface offset and deposit ages estimated from calcic soil development, are 0.02–0.05 mm/yr for the Levan segment and 0.01–0.03 mm/yr for the Fayette segment (data from the SE strand). Using the minimum net geomorphic surface offset calculated for the large scarp at the north end of the SW strand of the Fayette segment gives an estimated minimum long-term vertical slip rate of 0.06–0.1 mm/yr. The higher slip rate on this part of the fault may result from spillover of Levan-segment ruptures onto the Fayette segment, or additive slip from separate SW- and SE-strand Fayette-segment ruptures that overlap on this part of the fault, or some combination of these two scenarios. Additionally, the higher slip rate may reflect a

component of aseismic deformation resulting from localized diapirism or dissolution-induced subsidence associated with subsurface evaporite beds in the Middle Jurassic Arapian Shale.

In addition to the Levan and Fayette segments, we mapped Quaternary faults along the eastern base of the Valley Mountains, herein named the Dover fault zone. These faults are clearly less active than the Wasatch fault to the east, and are expressed as geomorphically degraded, east- and west-facing scarps on Quaternary-Tertiary alluvial deposits.

INTRODUCTION

The Levan and Fayette segments are the two southernmost segments of the Wasatch fault zone (WFZ), the longest active normal-slip fault in the western United States and the most active fault in Utah. The Levan and Fayette segments extend through a rural area of low population density in central Utah, and therefore present less seismic risk than the central segments of the WFZ that extend through the heavily populated Wasatch Front. Nevertheless, the Levan segment shows evidence for late Holocene surface faulting, and part of the Fayette segment shows evidence for Holocene surface faulting. Detailed mapping of these segments provides the basis for accurately characterizing the relative contribution of this part of the WFZ to the seismic hazard of central Utah, and contributes to our understanding of the overall paleoseismic behavior of the WFZ. Additionally, this map completes 1:50,000-scale surficial geologic mapping of the entire length of the WFZ affected by Holocene surface faulting (figure 1).

The Levan and Fayette segments lie at the base of the western slope of the San Pitch Mountains (also known as the Gunnison Plateau) (figure 2). The Levan segment forms the eastern margin of southern Juab Valley and the Fayette segment forms the eastern margins of northern Sevier Valley and Flat Canyon. The Levan segment is expressed as a series of discontinuous scarps extending from 5 km south of the city of Nephi southward about 32 km to the Juab–Sanpete County line. The Fayette segment extends from 1.5 km north of Chriss Canyon in southern Juab County southward about 22 km to the town of Fayette in Sanpete County, and comprises three strands that join near the mouth of Hells Kitchen Canyon: a 12-km-long northern (N) strand, a 6-km-long southwestern (SW) strand, and a 10-km-long southeastern (SE) strand. Utah Highway 28 closely parallels the faults and crosses the SW strand of the Fayette segment. The Sevier River flows northward through Sevier Valley, and then

¹Utah Geological Survey, Salt Lake City, Utah

²U.S. Geological Survey, Denver, Colorado

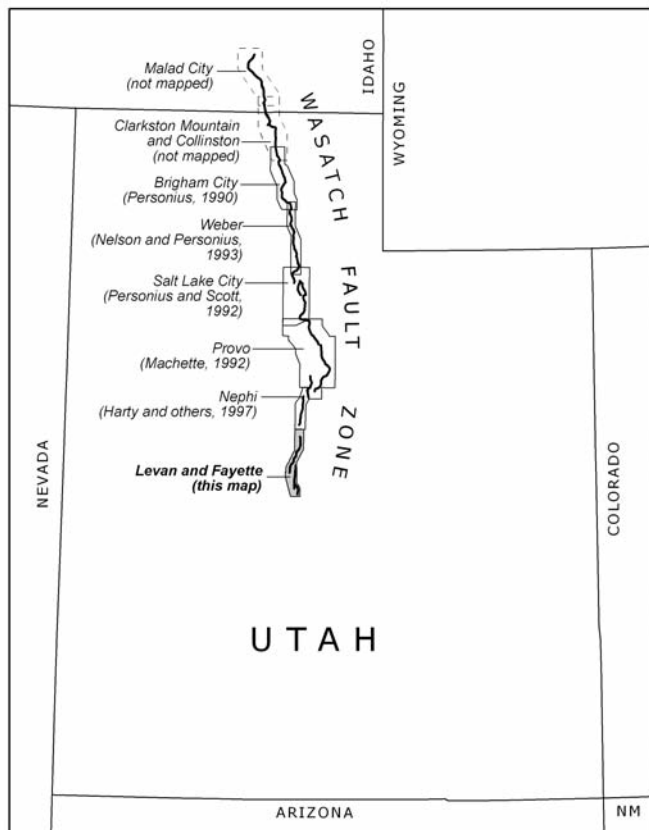


Figure 1. Index map of Wasatch fault zone showing segments (after Machette and others, 1992) and published 1:50,000-scale surficial geologic maps. Study of Clarkston Mountain and Collinston segments (Hylland, 2007a) did not include surficial geologic map.

turns westward near the southern end of the Levan segment. Sevier Bridge Dam (spillway elevation 1529 m; 5014 ft on base map), in southern Juab County, impounds water of the Sevier River to form Sevier Bridge Reservoir (also known as Yuba Lake), which periodically inundates the valley as far south as Fayette. The Valley Mountains form the western border of northern Sevier Valley.

The following discussion includes a brief summary of previous paleoseismic studies on the Levan and Fayette segments, a description of the methods used in this study, descriptions of Quaternary geologic deposits and fault scarps in the map area, estimates of the timing of surface-faulting earthquakes, descriptions of the segment boundaries, and estimates of late Quaternary slip rates. Metric (SI) units are used throughout this discussion except for elevations of map features (such as shorelines), which are reported using English units (feet) to be consistent with the base maps.

Previous Paleoseismic Studies

Previous paleoseismic studies on the Levan and Fayette segments include scarp profiling on both segments (Machette, unpublished mapping, 1984–86), examination of a natural exposure of the fault on the Levan segment at Deep Creek (Schwartz and Coppersmith, 1984; Machette, unpublished mapping, 1984–86; Jackson, 1991), and trenching of the Levan segment near Skinner Peaks (Jackson, 1991). Additionally, Crone (1983) and Schwartz and Coppersmith

(1984) reported radiocarbon ages of 2100 ± 300 and 1750 ± 350 ^{14}C yr B.P., respectively, for charcoal collected from faulted fan alluvium at Pigeon Creek on the Levan segment (figure 2), which helped constrain the timing of the most recent surface-faulting event (MRE). Machette and others (1992) summarized the results of these earlier studies.

Jackson (1991) logged the fault exposure at Deep Creek (figure 2) and calculated 1.8 m of net vertical tectonic displacement (NVTD) for the single scarp-forming earthquake, similar to the 1.75 m of NVTD measured by Machette (reported in Machette and others, 1992). Jackson (1991) also obtained a thermoluminescence (TL) age estimate of 1000 ± 100 yr for an organic soil horizon buried by scarp-derived colluvium. This age, which Jackson interpreted as a close maximum limit on the timing of the scarp-forming earthquake, is consistent with the maximum age of the scarp at Pigeon Creek as established by the charcoal ages of Crone (1983) and Schwartz and Coppersmith (1984). During reconnaissance mapping between Levan and Gunnison, Schwartz and Coppersmith (1984) obtained a radiocarbon age of 7300 ± 1000 ^{14}C yr B.P. (8300 ± 2300 cal yr B.P.; see appendix B, sample SC2) on charcoal from an unspecified position low in the footwall exposure at Deep Creek (Jackson, 1991, p. 9), providing a broad maximum limit on the timing of the scarp-forming earthquake and probably a broad minimum limit on the timing of any earlier event. However, given the limited depth of exposed hanging-wall deposits and the uncertainty of the charcoal-sample location, the exact significance of the radiocarbon age relative to penultimate-event (PE) timing is unclear.

At the Skinner Peaks trench site (figure 2), Jackson (1991) described evidence for two surface-faulting earthquakes on the Levan segment. He estimated a minimum and maximum NVTD of 2.0 ± 0.2 m and 2.8 ± 0.2 m, respectively, for the MRE, and a minimum NVTD of 0.8 m for the PE. Using a combination of TL and radiocarbon age estimates, Jackson (1991) determined that the MRE occurred around 1000–1500 cal yr B.P. (and closer to 1000 cal yr B.P.) and the PE occurred sometime before 3100 ± 300 to 3900 ± 300 cal yr B.P.

Methods

This map combines new surficial geologic mapping with compiled existing geologic quadrangle mapping (figure 3). Because documentation of late Quaternary faulting was not the primary purpose of the existing quadrangle maps, our new mapping focused on the relations between Quaternary deposits and fault scarps along the Levan and Fayette segments. Our mapping, which included reconnaissance field mapping by Machette in 1984 and detailed aerial-photograph and field mapping by Hylland in 2003–04, made use of 1:20,000-scale black-and-white aerial photographs (1965, U.S. Department of Agriculture) and lineament maps generated from low-sun-angle aerial photography (Cluff and others, 1973). U.S. Soil Conservation Service maps (Swenson and others, 1981; Trickler and Hall, 1984) aided in differentiating gradational alluvial-fan and lacustrine deposits. In addition to mapping along the WFZ, we extended our mapping to the west side of the Sevier River flood plain to encompass other Quaternary faults and previously unmapped Lake Bonneville deposits.

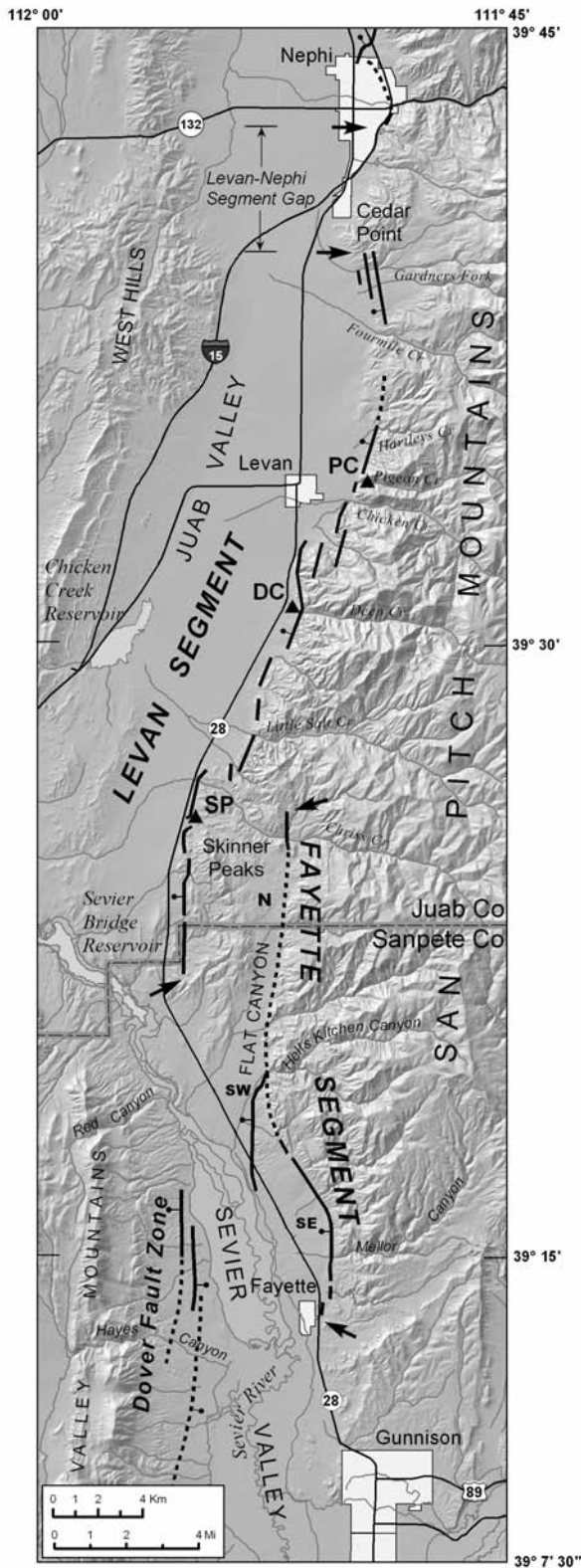
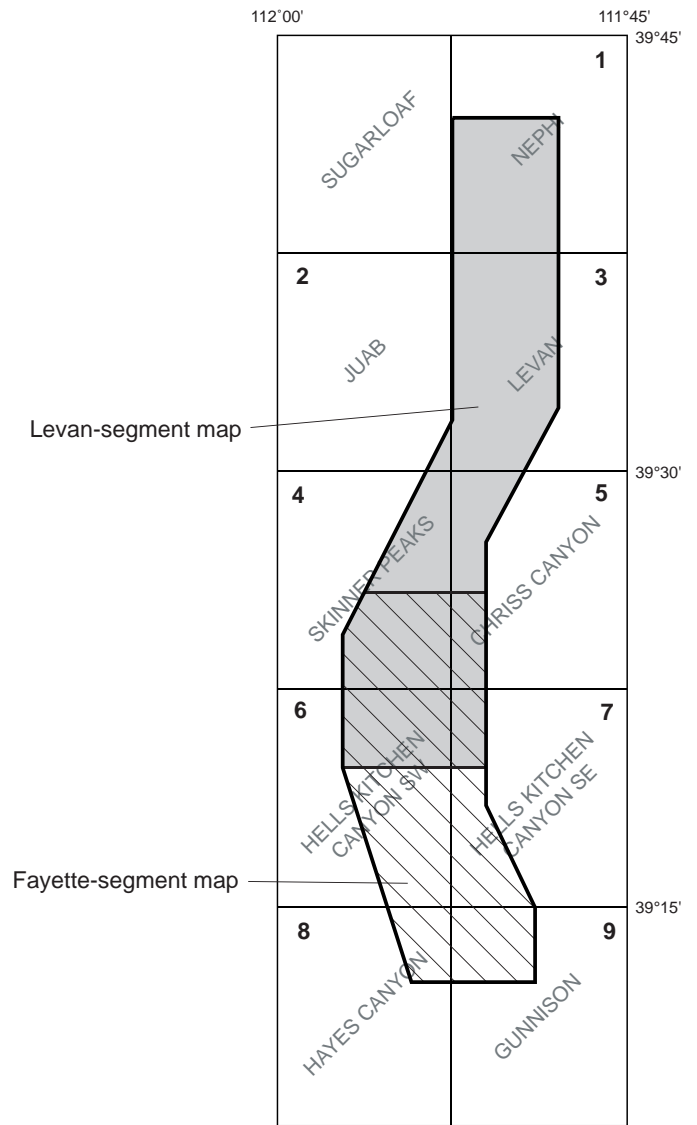


Figure 2. Levan and Fayette segments of the Wasatch fault zone. Strands of Fayette segment identified as N (northern), SW (southwestern), and SE (southeastern). Generalized Quaternary fault traces shown by heavy lines, dotted where concealed, bar and ball on down-thrown side; arrows show ends of segments. Paleoseismic study sites on Levan segment shown by triangles: PC, Pigeon Creek (former natural exposure); DC, Deep Creek (natural exposure); SP, Skinner Peaks trench (Jackson, 1991). Dover fault zone (named in this study) also shown.



Sources of geologic data:

1. Biek (1991)
2. Clark (1990)
3. Auby (1991)
4. Felger and others (2007)
5. Weiss and others (2003)
6. Witkind and others (1987)
7. Mattox (1987)
8. Petersen (1997)
9. Mattox (1992)

Figure 3. Index of map coverage relative to USGS 7.5-minute quadrangles, sources of compiled geologic data, and areal extent of individual segment maps on plate 1.

The map-unit symbols used herein generally follow the basic conventions used on the previously published surficial geologic maps of the other WFZ segments (figure 1). Detailed descriptions of the map units are given in appendix A. We differentiate Quaternary geologic units using standard relative-age criteria such as geomorphic expression, landform preservation, stratigraphic position, and soil development. For carbonate morphology in soils, we used the profile-development descriptions and stage classification summarized in Machette (1985a) and Birkeland and others (1991). Several numerical ages for bulk soil and detrital charcoal, including three radiocarbon ages obtained during this study, constrain the age of Holocene alluvial-fan deposits. Appendix B summarizes details of the radiocarbon analyses and conversion to calendar-calibrated ages.

We used morphometric fault-scarp data to evaluate the number and timing of scarp-forming earthquakes and to calculate long-term geologic (average) vertical slip rates. Appendix C shows the scarp-profile locations and data, and Hylland (2007b) discussed details of the data, analyses, and interpretation. Figure 4 summarizes terminology used to describe fault-scarp morphology.

QUATERNARY DEPOSITS AND DEPOSITIONAL HISTORY

Relative uplift of the San Pitch and Valley Mountains since late Tertiary time has been accompanied by deposition of basin fill in Juab and Sevier Valleys, including widespread piedmont-slope fan alluvium along the Levan and Fayette segments. Lake Bonneville occupied southernmost Juab Valley and the northern part of Sevier Valley for a relatively short period during the late Pleistocene, and scattered deposits of fine-grained lacustrine sediment remain. Other Quaternary deposits present locally in the map area include stream alluvium, landslide and debris-flow deposits, colluvium and talus, and eolian deposits.

Alluvial Deposits

Bouldery alluvial-fan deposits of Pleistocene to possibly Miocene age (unit QTaf) are preserved mostly in the segment-boundary areas of the Levan and Fayette segments, and also at the foot of the Valley Mountains in the vicinity of Red

Canyon (figure 5). At the northern end of the Levan segment, Auby (1991) and Biek (1991) referred to these deposits as the Salt Creek Fanglomerate. Biek (1991) and Felger (1991) noted that the deposits on the east side of Juab and Sevier Valleys may include erosional material that records the initial uplift of the Gunnison Plateau (San Pitch Mountains). The surfaces of these deposits are generally strewn with carbonate rubble derived from weathered calcic paleosol horizons and are typically as much as 150 m above the adjacent valley floor, but locally are as much as 300 m above the floor of Juab Valley (Auby, 1991). About 2 km south of Hells Kitchen Canyon, the surface of a small remnant of unit QTaf is tilted gently back to the east, toward the mountain front, presumably due to block rotation resulting from fault movement on the SW and SE strands of the Fayette segment.

Quaternary-Tertiary basin-fill deposits (unit QTab) are locally exposed near the Yuba State Park (Painted Rocks) boat ramp on the east shore of Sevier Bridge Reservoir (figure 6), and on the horst block of the Dover fault zone (see "Other Fault Scarps on Quaternary Deposits") along the base of the Valley Mountains south of Red Canyon. The deposits consist of light brown to reddish brown, weakly to moderately consolidated clay, silt, and sand with interbedded pebble to cobble gravel. South of Red Canyon, exposures locally reveal a calcic paleosol of unknown thickness having stage IV (laminar) carbonate morphology (for example, along the dirt road in the NE1/4 section 28, T. 18 S., R. 1 W.). These deposits may correlate, at least in part, with the Axtell Formation (Spieker, 1949) and/or Sevier River Formation (Callaghan, 1938; see also Anderson and Rowley, 1975). As a whole, unit QTab represents relatively low-energy basin-floor deposition with sporadic, higher energy deposition associated with ancestral Sevier River channel migration.

We correlate QTaf and QTab deposits with similar deposits in the Mills Valley area northwest of Sevier Bridge Dam (Oviatt, 1992; Oviatt and Hintze, 2005). There, silicic volcanic ash layers interbedded with fan alluvium and contemporaneous fine-grained basin-fill deposits have been geochemically correlated with ashes of known age, including the Lava Creek B, Bishop, Bear Creek, and Alturas ashes, and thus span the time period from 0.62 to 4.8 Ma (Oviatt, 1992). Reversed polarity of the ashes that correlate with the Bear Creek and Alturas ashes, indicating deposition prior to the Brunhes-Matuyama chron boundary (0.78 Ma; Baksi and others, 1992), is consistent with ages of 2.0 and 4.8 Ma, re-

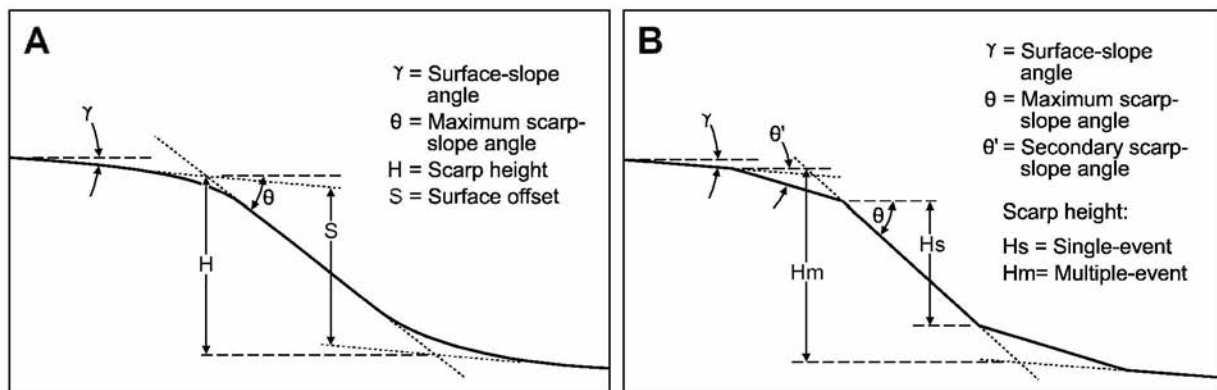


Figure 4. Schematic diagrams illustrating fault-scarp nomenclature used in this report. (A) Single-event scarp (modified from Bucknam and Anderson, 1979). (B) Multiple-event scarp (modified from Machette, 1982).



Figure 5. Quaternary-Tertiary alluvial-fan deposits (unit QTaf) exposed on east side of the Sevier River south of Yuba State Park (SE1/4 section 21, T. 17 S., R. 1 W.). Paleochannel incised into sandy/gravelly alluvium is filled with coarse, poorly sorted debris-flow deposits. Rock hammer for scale.



Figure 6. Quaternary-Tertiary basin-fill deposits (unit QTab) exposed next to the boat ramp at Yuba State Park (Painted Rocks; SE1/4 section 5, T. 17 S., R. 1 W.). Deposits consist of interbedded gravelly channel alluvium and silty flood-plain alluvium. Tilting of strata probably due to movement on intrabasin normal faults. Rock hammer for scale.

spectively (Oviatt, 1992). The ashes, therefore, indicate a minimum age span for these deposits of middle Pleistocene to early Pliocene. However, outcrops near the Yuba State Park (Painted Rocks) boat ramp reveal faulting and tilting of the QTab deposits and an angular unconformity between the QTab and QTaf deposits. These relations indicate that at least locally, unit QTab is older than unit QTaf, and may be no younger than early Pleistocene.

A veneer of pediment-mantle alluvium (unit ap) overlies a relatively planar, dissected surface of erosion along the eastern base of the Valley Mountains south of Red Canyon. The deposits unconformably overlie Quaternary-Tertiary basin-fill and alluvial-fan deposits, and possibly Tertiary bedrock at their westernmost extent, and are as much as 30 m above adjacent drainages. On the horst block of the Dover fault zone (see "Other Fault Scarps on Quaternary Deposits"), the pediment-mantle alluvium is very thin and discontinuous, probably as a result of uplift-induced erosion. The pediment and associated alluvial deposits are part of a regionally extensive surface present along most of the eastern base of the Valley Mountains (see Willis, 1988, 1991; Petersen, 1997).

Along the range fronts, upper Quaternary fan alluvium deposited prior to the Bonneville lake cycle (units af4 and afo) is generally preserved in relatively small, isolated remnants whose surfaces are about 5–15 m above adjacent younger alluvial fans and modern stream channels. Relatively large and more continuous surfaces are preserved on the structural block between the SW and SE strands of the Fayette segment. Soil carbonate development in the upper part of the alluvium ranges from continuous, thin to relatively thick coatings of secondary CaCO₃ on clasts (stage II carbonate morphology) to a continuous horizon of completely cemented CaCO₃ having a weak platy to laminar structure (stage III+ to stage IV). Surfaces underlain by pre-Bonneville fan alluvium are typically strewn with carbonate rubble derived from weathered calcic paleosol horizons. The pre-Bonneville fan alluvium was deposited around 100–250 ka (late to middle Pleistocene) based on comparison with soil carbonate morphology in the Beaver basin, about 110 km southwest of Fayette but in a similar climatic zone (table 1) and where Machette (1985a, 1985b) determined rates of secondary CaCO₃ development and soil ages.

Deposition of fan alluvium continued during and after the Bonneville lake cycle as part of a regional, probably climate-controlled, period of rapid and extensive fan sedimentation during the latest Pleistocene to middle Holocene (see,

for example, Christenson and Purcell, 1985; Keaton and others, 1991; Machette, 1992; Machette and others, 1992). West of the Sevier River, unit afb appears to have been deposited by streams graded to a transgressing Lake Bonneville and its highest shoreline (18–16.8 ka; see discussion below under "Lacustrine History and Related Deposits"). East of the Sevier River and in Juab Valley, fan deposits lack direct association with lacustrine deposits, but likely postdate the Bonneville lake cycle based on geomorphology and soil development. Unit af2 underlies isolated surfaces that are as much as 5 m above adjacent younger alluvial fans and modern stream channels. Thin, discontinuous to continuous CaCO₃ coatings are present on the undersides of clasts (stage I+), indicating these deposits probably range in age from middle Holocene to latest Pleistocene. The youngest deposits (unit af1) form small, discrete alluvial fans where depositional processes are still active. Surface gradients of these fans range from about 3° to 10°, and the deposits grade downslope into coalesced fan alluvium (unit afc). Active alluvial deposition also occurs on the low-gradient (1.5°–3°) coalesced alluvial fans that form broad bajadas in Juab Valley and along the eastern part of Sevier Valley and Flat Canyon, although modern deposition is restricted mostly to the proximal parts of these fans near the mountain front. Much of the remainder of the near-surface layers of these deposits probably accumulated during the early Holocene and latest Pleistocene. Exposures of coalesced fan alluvium are rare, but a stream cut along Fourmile Creek in the NE1/4NW1/4 section 5, T. 14 S., R. 1 E. exposes a 3-m-thick sequence of sandy alluvial deposits and interbedded eolian silt. The deposits at this locality are likely mid-Holocene in age based on stage I carbonate morphology and the presence of a weakly developed Bt soil horizon.

Although we have correlated the various Quaternary alluvial-fan deposits of Juab Valley with those of Sevier Valley to the south, the actual ages of the fan surfaces may differ between the two valleys. Southern Juab Valley has no axial trunk stream, and with the exception of its extreme southern end, was not inundated by Lake Bonneville. Base-level change for streams flowing into Juab Valley, therefore, has been dominated by a slow rise associated with ongoing aggradation of basin fill, and fan incision and surface abandonment are governed by surface faulting and climatically controlled changes in stream flow. In contrast, Sevier Valley has an axial trunk stream, the Sevier River, and waters of Lake Bonneville filled the northern part of the valley to a depth of at least 25 m. Therefore, in addition to the factors

Table 1. Comparison of climatic factors influencing rates of calcic soil development between locales in the map area (Nephi, Levan, Gunnison) and Beaver, Utah.

| Location | Mean Annual Precip. (cm) | Mean Annual Max. Temp. (°C) | Mean Annual Min. Temp. (°C) | Period of Record ¹ |
|---------------------|-----------------------------|--------------------------------|--------------------------------|-------------------------------|
| Beaver ² | 29 | 17.6 | -0.6 | 1890–1990 |
| Nephi | 37 | 18.7 | 2.4 | 1941–2004 |
| Levan | 36 | 17.3 | 1.3 | 1895–2004 |
| Gunnison | 23 | 18.5 | -0.5 | 1956–1990 |

¹Data from Western Regional Climate Center (undated).

²Location of detailed soil study by Machette (1985a, 1985b).

described above for Juab Valley, fan incision and surface abandonment in northern Sevier Valley have also been controlled by fluctuations in base level associated with changes in the longitudinal profile of the Sevier River and the presence or absence of Lake Bonneville.

Stream alluvium is present as channel and flood-plain deposits, a broad alluvial apron in the area of Old Pinery Canyon and Gardners Fork at the northern end of the Levan segment, and undifferentiated basin fill in interior valley-floor areas. Older stream alluvium (unit alo) in the Old Pinery Canyon–Gardners Fork area forms a thick alluvial apron that extends into Juab Valley, forming a drainage divide known as Levan Ridge. The streams supplying sediment to Levan Ridge appear to be grossly underfit, and most of the alluvium of Levan Ridge may have been deposited by a paleo-channel of Salt Creek, possibly diverted to its present location east of the town of Nephi by stream capture as recently as the late Pleistocene (Machette and others, 1992). Surfaces underlain by older stream alluvium are as much as 40 m above modern streams. These surfaces are typically strewn with carbonate rubble derived from weathered calcic paleosol horizons, and we correlate these stream-alluvium deposits with the pre-Bonneville fan alluvium of late to middle Pleistocene age. Intermediate-age stream alluvium (unit al2) typically forms terraces as much as 5 m above modern streams and has soils with stage I to stage II carbonate morphology; we interpret these deposits to be middle Holocene to latest Pleistocene in age. The youngest stream alluvium (unit al1) represents late Holocene deposition in modern stream channels and flood plains. Fine-grained, Holocene flood-plain alluvium of the Sevier River (unit alsr) is present in the middle of Sevier Valley. These deposits include reworked Lake Bonneville sediments as well as lacustrine silt and clay deposited during times when the valley floor is inundated by Sevier Bridge Reservoir. Minor, shallow drainages and basins contain stream alluvium mixed with a significant component of hillslope colluvium (unit ac). Finally, where alluvial fans are poorly developed or absent in the southern part of Juab Valley, in the interior part of Sevier Valley, and in the western part of Flat Canyon, we map the valley-floor deposits as undifferentiated basin-fill alluvium (unit ab).

Two aspects of the Sevier River channel and flood plain in northern Sevier Valley may have tectonic significance. First, the majority of abandoned channels and oxbow lakes lie west of the modern channel, indicating eastward channel migration during the Holocene. Keaton (1987) observed a similar eastward migration of the Jordan River in Salt Lake Valley, on the hanging wall of the Salt Lake City segment of the WFZ, and postulated that the pattern could be the result of migration away from the center of post-Lake Bonneville isostatic rebound (Crittenden, 1963), tectonic subsidence associated with faulting, or both. Second, the modern flood plain narrows dramatically in the vicinity of Red Canyon. Here, the Sevier River cuts across the large Red Canyon alluvial fan (unit QTaf), isolating the toe of the fan on the east side of the river. The river must have followed a more eastern course during the time when the fan was forming, flowing around the toe of the fan. Apparently, the combined effects of lateral erosion and migration of the Sevier River channel and headward erosion of distributary channels on the fan during the early or middle Pleistocene, perhaps facilitat-

ed by surface faulting, eventually resulted in capture of the Sevier River and rerouting of the channel across the alluvial-fan deposits. Subsequent deposition of basin-fill sediment has filled in parts of the former channel and produced the shallow closed depression west of Highway 28 near the mouth of Flat Canyon.

Lacustrine History and Related Deposits

A shallow arm of late Pleistocene Lake Bonneville occupied the southernmost part of Juab Valley and the northern part of Sevier Valley during the Bonneville-level highstand at 18–16.8 ka. As summarized by Currey (1990) and Oviatt and others (1992), the Bonneville lake cycle began around 30 ka. Over time, the lake rose and eventually reached its highest level at the Bonneville shoreline around 18,000 cal yr B.P. (see Biek and others, 2007, for calendar calibration of radiocarbon-based shoreline ages used in this discussion). At the Bonneville level, lake water overflowed the low point on the basin rim at Zenda in southeastern Idaho, spilling into the Snake–Columbia River drainage basin. Around 16,800 cal yr B.P., the alluvial-fan deposits at the Zenda outlet failed catastrophically, resulting in a rapid drop in lake level of approximately 110 m associated with the Bonneville Flood. The lake level stabilized when further erosional downcutting was essentially stopped by the bedrock-controlled Red Rock Pass threshold. The lake remained at or near this level for about 2500 years (Godsey and others, 2005), forming the Provo shoreline. A change in climate to warmer and drier conditions caused the lake to regress rapidly from the Provo shoreline to near modern Great Salt Lake levels by the end of the Pleistocene.

Assuming present valley-floor elevations are not substantially higher than valley-floor elevations at the onset of lacustrine sedimentation, and using Currey's (1990) Lake Bonneville hydrograph, lake water was present in the map area for a period of about 3000 years leading up to the Bonneville Flood (figure 7). The lowest elevations in the map area are above the elevation of the Provo shoreline, so only the Bonneville shoreline is present. The shoreline is best expressed as a wave-cut bench on the dip slope of Eocene tuff on the west side of the Painted Rocks (NW1/4 section 5, T. 17 S., R. 1 W.); Crittenden (1963) determined an elevation of 5090 ± 5 ft (1551–1554 m) for the shoreline here. This area was likely a focus for relatively high wave energy associated with winds out of the south and west. Currey (1982) reported a local Bonneville shoreline erosional platform approximately 7 km northwest of Fayette at an elevation of 1556 ± 2 m (5097–5110 ft). Elsewhere in the map area, topographic expression of the shoreline is absent, probably due to a combination of low valley-floor topographic gradients and generally quiet water.

Below the elevation of the Bonneville shoreline, discontinuous deposits of mostly fine-grained lacustrine sediment are present on both sides of the Sevier River flood plain. The deposits generally consist of thin- to thick-bedded silt, clay, and fine sand containing bivalve and gastropod shells, and were deposited in an underflow-fan type of deltaic environment as northern Sevier Valley was gradually inundated during transgression of the lake to the Bonneville highstand. Oviatt (1987, 1989) applied the underflow-fan concept (wherein fine-grained clastic sediment is deposited in rela-

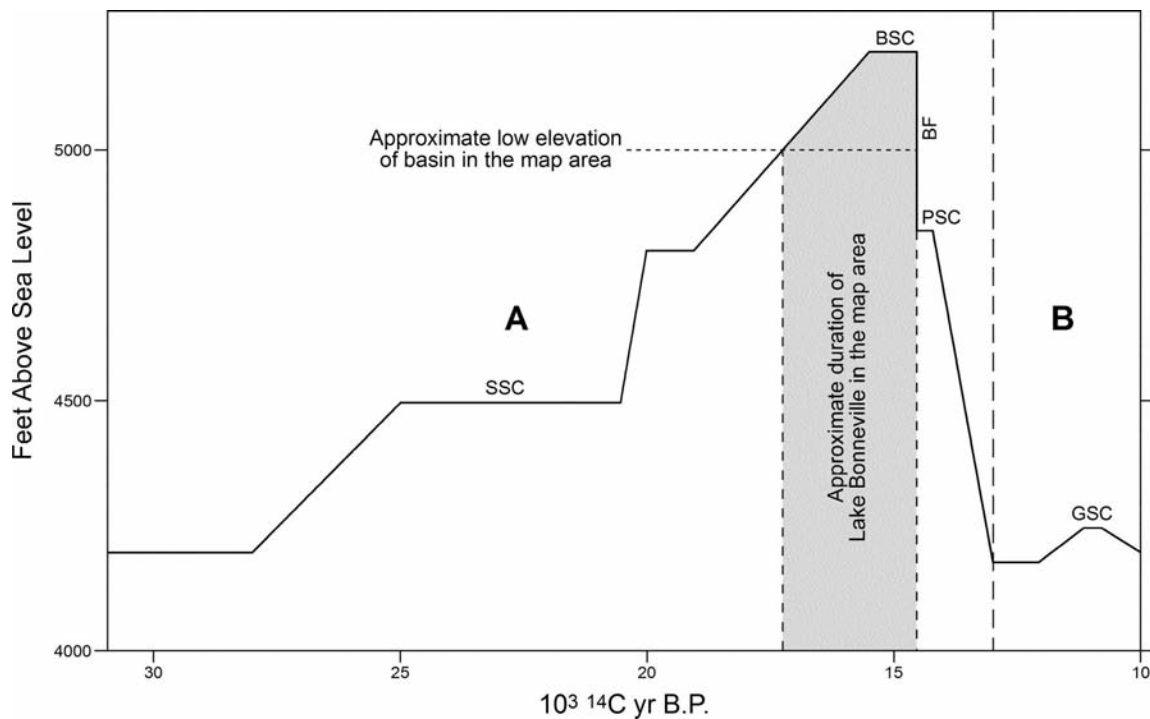


Figure 7. Schematic hydrograph of Bonneville basin during (A) the Bonneville paleolake cycle and (B) in early post-Bonneville time, showing approximate duration (~17,400 to 14,500 ^{14}C yr B.P.) of shallow arm of Lake Bonneville in the map area (modified from Currey, 1990). SSC, Stansbury shoreline complex; BSC, Bonneville shoreline complex; BF, Bonneville Flood; PSC, Provo shoreline complex; GSC, Gilbert shoreline complex.

tively shallow water by density currents at the mouth of a major river) to similar lacustrine deposits elsewhere in the Bonneville basin of central Utah, and that model of sedimentation is applicable here. Lacustrine silt and clay deposits (unit lbn), having little to no sand, are well exposed near the Yuba State Park (Painted Rocks) boat ramp (figure 8). The ground surface of unit lbn typically displays a polygonal pattern of shrinkage cracks, indicating the presence of expansive clay. Locally, the uppermost beds of the fine-grained deposits include thin beds of pebble gravel (unit lbn_g), probably deposited in a shoreline environment by tributary streams flowing into the lake during its highstand. Elsewhere, lacustrine sand deposits (unit lbs) consisting of well-sorted fine sand with interbedded silt and clay represent shallow-water nearshore/beach environments.

Small, scattered deposits of mostly Holocene-age, well-sorted, fine-grained eolian sand (unit es) are present near the Painted Rocks and at the south end of the Fayette segment. The sand probably consists largely of reworked Lake Bonneville sediment (Mattox, 1992). Some of these deposits form small dunes.

Colluvial and Mass-Movement Deposits

Colluvial and mass-movement deposits in the map area include hillslope and fault-scarp colluvium, deposits of mixed colluvium and alluvium, rock-fall and talus deposits, landslide deposits, and debris-flow deposits. Thin, discontinuous deposits of hillslope colluvium (unit chs) of late Pleistocene to Holocene age generally overlie bedrock throughout the map area. However, we mapped only deposits that are continuous over a relatively large area, and where relatively sig-

nificant (thick or widespread) accumulations also include an alluvial component (unit ca). We mapped fault-scarp colluvium (unit cfs) along the large (>20 m high) scarp near the north end of the SW strand of the Fayette segment, where the colluvium forms a wedge as much as 2 m thick on the down-dropped side of the fault (see figure 9B for an illustration of scarp-derived colluvium). Rock-fall and talus deposits (unit crf) of late Pleistocene to Holocene age are present mostly on the relatively steep slopes of Pigeon and Chicken Creeks east of Levan, where beds of fractured limestone are rock-fall source areas.

Relative ages of the landslide deposits are poorly constrained. They are based primarily on geomorphic expression and are intended to indicate relative timing of the initiation of movement or reactivation. Older (Pleistocene) landslide deposits (unit clso) include the Fourmile Creek landslide complex (Auby, 1991), which consists of a large (6.5 km²), stratigraphically disrupted, lithologically heterogeneous mass along the range front between Fourmile Creek and Hartleys Canyon. Auby (1991) recognized strata of the Pliocene-Pleistocene Salt Creek Fonglomerate, Eocene-Oligocene Goldens Ranch Formation, and Middle Jurassic Arapien Shale within the landslide complex. The landslide complex (1) lacks a well-defined source area, (2) probably developed relatively in-place as the result of local instability of post-Arapien strata on the flank of the Levan culmination (the broad, north- to northeast-trending, Arapien-cored anticlinorium that forms the principal structure of the northwestern San Pitch Mountains [Weiss and others, 2003; Felger and others, 2007]) rather than by significant translational movement, and (3) includes areas of active landsliding too small to map separately. Small, younger (Holocene to late Pleis-



Figure 8. Fine-grained Lake Bonneville deposits (unit *lbm*). (A) Exposure in bluff south of boat ramp at Yuba State Park (Painted Rocks; SE1/4 section 5, T. 17 S., R. 1 W.). (B) Detail of weakly bedded clay and silty clay exposed in the vertical bluff face. (C) Polygonal shrinkage cracks on ground surface, indicating presence of expansive clay.

tocene) landslide deposits (unit *clsy*) are scattered throughout the map area. We mapped individual upper Holocene debris-flow deposits (unit *cd1*) on range-front alluvial fans where the deposits are large enough to show at the map scale. Many of these deposits are immediately downslope of a fault scarp, and document relative uplift and incision of the upper part of the alluvial fan as a result of faulting.

QUATERNARY FAULTING

Fault scarps are present on Quaternary deposits along most, but not all, of the Levan segment, and on the southern half of the Fayette segment. The scarps are mostly on unconsolidated fan and stream alluvium, but locally are on bedrock. Along the Levan segment, the faulted alluvium can be generally characterized as follows: (1) at the north end of the segment—sandy pebble and cobble gravel, dominated by well-rounded quartzite clasts, (2) between Hartleys Canyon and Chriss Canyon—pebble gravel in a matrix of sand, silt, and clay, dominated by tabular clasts of shaly limestone, and (3) south of Chriss Canyon—sandy pebble and cobble gravel with silt and clay, dominated by subangular, felsic volcanic

clasts. Along the Fayette segment, the faulted alluvium is generally pebble gravel with scattered cobbles and boulders in a matrix of sand, silt, and clay. Geomorphically, the scarps along the Levan segment are relatively fresh looking whereas those along the Fayette segment are more weathered and degraded. The Levan-segment scarps have maximum scarp-slope angles of $\leq 32^\circ$ and are generally in the wash-controlled stage of development of Wallace (1977), although debris-slope processes may still be active on some of the steeper scarps. The Fayette-segment scarps have lower maximum scarp-slope angles ($\leq 24^\circ$) and are in the wash-controlled stage of development of Wallace (1977).

Levan Segment

Along the Levan segment, fault scarps on upper to middle Pleistocene fan alluvium (units *af4* and *afo*) are as much as 12 m high and are clearly the result of recurrent late Quaternary surface faulting. Hartleys Canyon, 4.3 km northeast of Levan, marks the boundary between fault scarps to the north that appear to be pre-Holocene in age and scarps to the south that formed fully or in part from surface faulting dur-

ing the Holocene. North of Hartleys Canyon, Quaternary surface faulting within the Fourmile Creek landslide complex is uncertain because fault scarps are difficult to differentiate from landslide scarps, and reactivated landslide movement may have obliterated pre-existing fault scarps. North of Fourmile Creek, fault scarps on upper to middle Pleistocene stream alluvium (unit alo) and Quaternary-Tertiary alluvial-fan deposits (unit QTaf) show no geomorphic evidence of young (Holocene) faulting. Subparallel fault scarps on the alluvial apron in the area of Old Pinery Canyon and Gardners Fork form a zone approximately 1 km wide; scarp heights here range from about 3 to 5 m, scarp-slope angles are low (12° – 14°), and the scarps have smooth, rounded crests—all indicating relatively old morphology and time of formation.

South of Hartleys Canyon, discontinuous Holocene fault scarps extend southward to the Juab–Sanpete County line. Between Hartleys Canyon and Chriss Canyon, fault scarps on Holocene deposits have a simple morphology and appear to have formed from a single surface-faulting event. Along this part of the segment, measured height of single-event scarps ranges from 0.9 to 4.3 m (average 2.7 ± 0.9 m), net geomorphic surface offset ranges from 0.5 to 2.0 m (average 1.6 ± 0.5 m), and maximum scarp-slope angle ranges from 17° to 32° (average $25^{\circ} \pm 5^{\circ}$) (appendix C; ranges and averages exclude data from profiles L68 and L71.1). In a few places, channels associated with intermittent streams that have breached the scarps have sharp knickpoints that have retreated less than 10 m from the scarps. Small antithetic scarps west of the main scarps form small grabens (less than 10 m wide) in many places, and cause stream channels to make an abrupt bend and follow the fault trace for a short distance. Net geomorphic surface offset across the zone of deformation is typically about 50% of the scarp height where a graben is present, and about 75% of the scarp height where a graben is not present.

South of Chriss Canyon, scarps on Holocene deposits are likely the result of two surface-faulting events, based on a composite morphology (bevel) apparent on many but not all of the scarp profiles from this area as well as stratigraphic data from the Skinner Peaks trench (Jackson, 1991). Along this part of the segment, measured scarp height ranges from 1.2 to 3.9 m (average 2.7 ± 0.9 m), net geomorphic surface offset ranges from 0.7 to 3.1 m (average 2.1 ± 0.8 m), and maximum scarp-slope angle ranges from 11° to 25° (average $19^{\circ} \pm 4^{\circ}$) (appendix C).

The Holocene fault scarps comprise several discrete geometric sections along the Levan segment as defined by fault terminations in bedrock and/or lateral step-overs to adjacent sections. From Hartleys Canyon, scarps on Holocene alluvial fans extend south-southwest about 6 km along the base of the roughly linear range front. About 2.5 km south of Levan, where the range front makes a bend to the south, the fault scarps make an en echelon right step across intrusive igneous bedrock, and scarps on Holocene alluvial fans continue south along the base of the range front for another 6 km to near Little Salt Creek. Here, the range front makes a shallow reentrant, and the fault zone steps left. Within the reentrant, Holocene fault scarps extend to the prominent unnamed drainage 1.5 km south of Little Salt Creek, where they terminate on bedrock north of Chriss Canyon. At Chriss Canyon, the fault zone again steps right, and scarps on

Holocene alluvial fans extend about 3 km along the range front to a point west of Skinner Peaks. From here, the range front to the south is less well defined, and Holocene scarps step left and continue about 4 km south in shallow basins that parallel the eastern margin of Juab Valley. At the southern end of the shallow basins, the fault scarps along this trend terminate on Tertiary volcanoclastic rocks. To the east, additional scarps are present on Quaternary-Tertiary alluvial-fan deposits (unit QTaf) in the Levan-Fayette segment boundary area (see discussion below under “Segment Boundaries”).

Stratigraphic relations exposed in the stream cut at Deep Creek show that the scarp there formed during a single faulting event (the Levan-segment MRE), and several lines of evidence from the scarp and stream-cut exposure of the fault indicate late Holocene timing for the scarp-forming earthquake. First, Schwartz and Coppersmith’s (1984) radiocarbon age of 7300 ± 1000 ^{14}C yr B.P. (8300 ± 2300 cal yr B.P.; see appendix B, sample SC2) on charcoal from the footwall exposure provides a broad maximum limit for the timing of the MRE. Second, scarp morphology and empirical analysis of morphometric scarp data indicate a late Holocene MRE (Machette and others, 1992; Hylland, 2007b). Finally, late Holocene timing has been confirmed by numerical dating of sediment from the natural exposure of the fault (figure 9). Jackson’s (1991) thermoluminescence (TL) age of 1000 ± 100 yr for the A horizon paleosol directly overlain by scarp-derived colluvium provides a close maximum limit on the timing of the MRE. As a check of this timing, we resampled the same horizon for radiocarbon dating of soil organics (sample L-DC-RC1; appendix B). The organic material produced an apparent mean residence time (AMRT) age of 1200 ± 80 ^{14}C yr B.P. (1000 ± 200 cal yr B.P.; appendix B), consistent with Jackson’s TL age and providing additional support for a surface-faulting earthquake sometime shortly after about 1000 cal yr B.P.

Stratigraphic data from the Skinner Peaks trench indicate the scarp there formed as the result of two surface-faulting events (Jackson, 1991), consistent with nearby scarps showing composite morphology (appendix C, profiles m72 to m84). Jackson determined the timing of surface faulting using a combination of TL and radiocarbon dating of organic sediment layers exposed in both the footwall and hanging wall. His estimate for timing of the MRE (between 1000 and 1500 cal yr B.P., and closer to 1000 cal yr B.P.) is consistent with the time of scarp formation at Deep Creek as well as at Pigeon Creek. For the timing of the PE, Jackson determined a minimum limit of between 3100 ± 300 yr B.P. (TL age) and 3900 ± 300 cal yr B.P. (charcoal age; reconverted in this study to 4000 ± 300 cal yr B.P. [appendix B]).

In an attempt to provide numerical age control on the timing of surface faulting along the Levan segment south of the Skinner Peaks trench site, we collected organic soil material and detrital charcoal from faulted fan alluvium (unit afy) exposed in a shallow gully incised into the footwall of the fault near Skinner Peaks (samples L-SP-RC1 and L-SP-RC2; appendix B). The samples produced stratigraphically consistent ages of 1500 ± 100 and 3500 ± 200 cal yr B.P., indicating late Holocene alluvial deposition on the footwall of the fault. Because the scarps on the southern part of the segment apparently did not form entirely as the result of a single surface-faulting earthquake around 1000 years ago (the MRE), the radiocarbon ages indicate that alluvial depo-

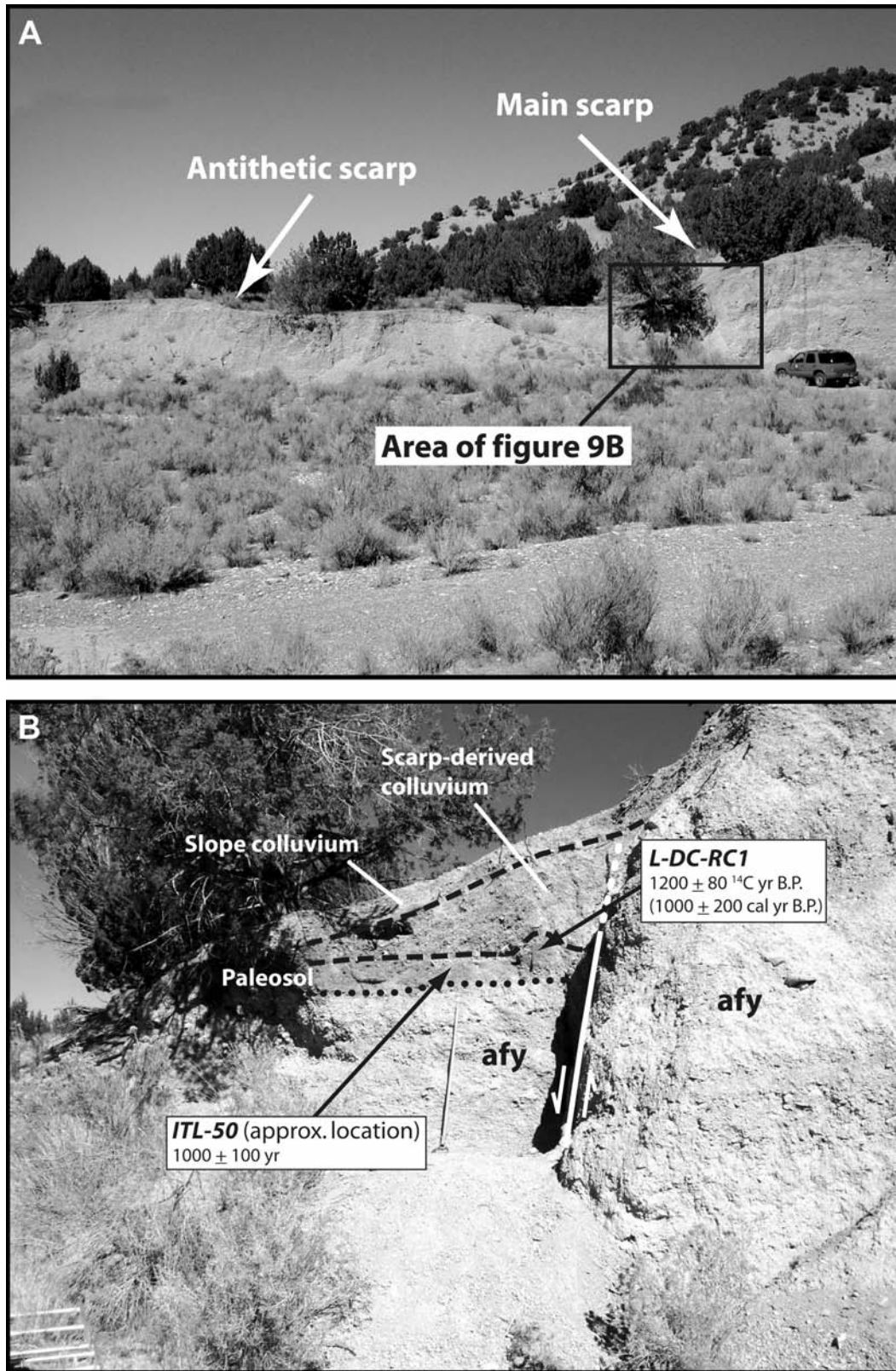


Figure 9. Deep Creek natural exposure of the Levan segment of the Wasatch fault zone (view looking north). (A) Fault zone consists of a 3.2-m-high west-facing main scarp and 0.5-m-high antithetic scarp that form a 30-m-wide graben. (B) Fault (white line) offsets post-Bonneville fan alluvium (unit afy). Presence of a single unfaulted wedge of scarp-derived colluvium indicates a single surface-faulting event. Thermoluminescence sample ITL-50 (Jackson, 1991) and radiocarbon sample L-DC-RC1 (this study) yielded numerical ages that indicate scarp formation shortly after about 1000 years ago. Handle of scraping tool is 1.4 m long.

sition continued on the footwall part of the fan after an earlier surface-faulting event (the PE) (i.e., the footwall fan surface was not abandoned as the result of relative uplift during the PE). Although these radiocarbon ages provide insight into the age of the fan alluvium, they do not necessarily constrain the timing of scarp formation because a clear stratigraphic and structural relation between the sampled deposits and the fault is lacking.

Fayette Segment

Late Quaternary fault scarps are relatively continuous along the southern half of the Fayette segment (SW and SE strands), but we observed no fault scarps on Quaternary deposits along the range front north of Hells Kitchen Canyon (N strand). However, Machette and others (1992) suspected that the range front in this area is fault controlled. Also, at the north end of Flat Canyon, Quaternary-Tertiary alluvial-fan deposits (unit QTaf) appear to be faulted down-to-the-west against Tertiary sedimentary strata (Weiss and others, 2003), indicating possible early or middle Pleistocene surface faulting. Therefore, the N strand of the Fayette segment has apparently undergone Quaternary surface faulting but has been inactive in late Quaternary time.

Fault scarps on the SW and SE strands of the Fayette segment include low (probably single-event) scarps on fan surfaces (unit af2) and stream terraces (unit al2) that range in age from latest Pleistocene to possibly middle Holocene. Geomorphically, these scarps appear to be older than comparable scarps on the Levan segment, and post-faulting alluvial-fan deposits (unit af1) on the hanging wall partially bury the scarps in places. Some of these scarps have a slight bevel, but we believe this is more likely due to erosional characteristics of the faulted alluvium, possibly related to calcic soil development, than to recurrent surface faulting.

Along the SW strand, measured height of inferred single-event scarps ranges from 1.5 to 2.6 m (average 2.0 ± 0.4 m), net geomorphic surface offset ranges from 0.8 to 1.6 m (average 1.2 ± 0.3 m), and maximum scarp-slope angle ranges from 16° to 25° (average $20^\circ \pm 4^\circ$) (appendix C; ranges and averages exclude data from profile m88). Along the SE strand, measured height of single-event scarps ranges from 1.2 to 2.9 m (average 1.7 ± 0.7 m), net geomorphic surface offset ranges from 0.5 to 1.3 m (average 0.9 ± 0.3 m), and maximum scarp-slope angle ranges from 7° to 15° (average $11^\circ \pm 3^\circ$) (appendix C). Where scarps on the SW and SE strands have similar height, the SE-strand scarps consistently have lower maximum scarp-slope angles, implying an earlier time of formation.

Some fault scarps on the Fayette segment are high, multiple-event scarps on upper to middle Pleistocene fan alluvium (units af4 and afo). Measured height of these scarps generally ranges from 4.3 to 5.6 m, and net surface offset generally ranges from 2.7 to 3.2 m. However, the scarp at the north end of the SW strand locally reaches a height of 22 m, and surface offset is at least 14 m. Actual offset is more, because the hanging wall has been buried by an unknown thickness of the adjacent Hells Kitchen Canyon alluvial fan (unit afc).

Numerical ages are lacking for Quaternary deposits along the Fayette segment, so the timing of surface faulting is only qualitatively constrained by soil-profile development,

geomorphology, and cross-cutting relations. Along both the SW and SE strands of the fault, lower(?) Holocene to upper Pleistocene fan and stream alluvium (units af2 and al2) is faulted, but upper Holocene alluvium (unit af1) is not. Also, Lake Bonneville deposits (unit lbs) at the south end of the SW strand appear to be faulted, although the suspect scarp is subtle. These relations indicate a post-Bonneville-highstand (<16.8 ka) and pre-late Holocene time for the MRE on the Fayette segment (see also Machette and others, 1992). Empirical analysis of scarp-profile data indicates a more recent (Holocene) MRE on the SW strand and an earlier (latest Pleistocene) MRE on the SE strand (Hylland, 2007b).

Other Fault Scarps on Quaternary Deposits

Within the Levan-Fayette segment-boundary area are numerous north- and northeast-trending fault scarps and lineaments on Quaternary-Tertiary alluvial-fan deposits (unit QTaf) and undifferentiated Quaternary basin fill (unit ab). These subsidiary structures appear to accommodate a left-stepping transfer of displacement between the main traces of the two segments. The scarcity of Holocene deposits in this area makes it difficult to evaluate recency of surface rupture, and late Quaternary surface faulting cannot be ruled out.

Along the west margin of northern Sevier Valley, a north-south-trending zone of fault scarps is present on Quaternary-Tertiary alluvial-fan deposits and undifferentiated basin fill (units QTaf and QTab) and the thin, overlying pediment-mantle alluvium (unit ap). We herein name these faults the Dover fault zone, for the former town site located near the scarps at the south end of the map area. The scarps, several of which were previously mapped by Petersen (1997), form a narrow zone on-trend with the south end of the Levan segment and the Levan-Fayette segment-boundary scarps and lineaments. The most prominent scarp is west of the Sanpete Fish and Game Club along the boundary of sections 15 and 16, T. 18 S., R. 1 W. This east-facing scarp ranges in height from 5 to 15 m and has a rounded crest and overall degraded morphology. A parallel, geomorphically similar, west-facing scarp is present about 0.5 km to the west, forming a narrow horst along which the power-line right-of-way is located. Numerous channels have been eroded across the horst by eastward-flowing streams, and no fault scarps are present on the Holocene alluvium (units al1, af1, and afy) deposited by the antecedent streams. Petersen (1997) interpreted the western fault as extending at least 2 km south of Hayes Canyon, and the eastern fault continuing (but concealed) to the south end of the Hayes Canyon quadrangle, south of the present map area (refer to figures 2 and 3). Petersen (1997) depicted the eastern fault as being a major range-bounding structure having approximately 4000 ft (1220 m) of vertical offset in undifferentiated Quaternary-Tertiary deposits, but the basis for this estimate is uncertain. The timing of most recent surface faulting on the Dover fault zone is uncertain, but scarp morphology indicates the faults may have been active in the early or middle Pleistocene.

SEGMENT BOUNDARIES

Under the earliest segmentation models of the WFZ, the Levan segment was defined as extending 40 km from east of

Levan southward to near Gunnison, and the Fayette segment was not identified as a segment of its own (Schwartz and Coppersmith, 1984). Based on recency of faulting and fault geometry, Machette and others (1991, 1992) subsequently divided the original Levan segment into the Levan segment (restricted sense; used herein) and the Fayette segment to the south.

Levan-Nephi Segment Boundary

Machette and others (1991, 1992) described a 15-km-long gap in Holocene faulting between the south end of the Nephi segment and north end of the Levan segment, and Machette and others (1992) placed the northern boundary of the Levan segment in the area of Hartleys Canyon. Although Hartleys Canyon marks the northernmost Holocene fault scarps on the segment, we suspect that Quaternary (possibly Holocene) surface faulting extended northward but is unrecognized within the Fourmile Creek landslide complex. Also, fault scarps are present on upper to middle Pleistocene alluvium (unit alo) in the area of Gardners Fork and Old Pinery Canyon (Biek, 1991; Machette and others, 1991, 1992; this map). These fault scarps terminate to the north on Quaternary-Tertiary alluvial-fan deposits (unit QTaf) on the southern slopes of Cedar Point in section 28, T. 13 S., R. 1 E. To the north, in the NW1/4 section 21, T. 13 S., R. 1 E., short escarpments are present on an isolated remnant of upper to middle Pleistocene fan alluvium (unit afo), but we are uncertain whether these were formed by faulting or erosion. Otherwise, no unambiguous evidence of Quaternary faulting exists between Cedar Point, which forms a minor salient in the range front, and the Holocene fault scarps that mark the southern end of the Nephi segment at the town of Nephi (Machette and others, 1992; Harty and others, 1997; figure 2). We propose that the northern boundary of the Levan segment be placed in the area of Cedar Point based on the 5-km-long gap in Quaternary faulting and range-front geometry described above.

Levan-Fayette Segment Boundary

The segment boundary area between the south end of the Levan segment and north end of the Fayette segment is a left-stepping area of overlap about 10 km long and 4 km wide; this area contains the north- and northeast-trending fault scarps and lineaments described above under "Other Fault Scarps on Quaternary Deposits." Holocene fault scarps on the Levan segment end about 0.5 km east of Utah Highway 28 near the southern jog in the Juab-Sanpete County line (section 4, T. 17 S., R. 1 W.). The N strand of the Fayette segment is present 4 km to the east, along the eastern margin of Flat Canyon. As described above under "Quaternary Faulting," we observed no scarps on Quaternary deposits along the range front of the San Pitch Mountains north of Hells Kitchen Canyon, but the range front in this area is likely fault controlled. At the north end of Flat Canyon and on-trend with the concealed range-front fault, fault juxtaposition of Quaternary-Tertiary alluvial-fan deposits against Tertiary sedimentary strata indicates possible early or middle Pleistocene surface faulting. This fault terminates in Tertiary bedrock about 1.5 km north of Chriss Canyon (SE1/4 section 12, T. 16 S., R. 1 W.), and we interpret this to be the northern end of the Fayette segment.

Weiss and others (2003) and Felger and others (2007) inferred a concealed fault in northwest-trending Chriss Canyon that juxtaposes Quaternary-Tertiary alluvial-fan deposits in the downthrown southern block against Tertiary sedimentary strata in the upthrown northern block. Weiss and others (2003) interpreted this fault as an oblique connecting structure between the Levan and Fayette segments. Like the N strand of the Fayette segment, there are no scarps on Quaternary deposits along this fault; however, if the fault trace is along the floor of the narrow canyon, any scarp formed there would be quickly obliterated by stream flow and sediment deposition. This concealed fault, together with the N strand of the Fayette segment, may have been active in early or possibly middle Pleistocene time, but likely has been inactive since then as activity shifted to the more northeasterly-trending faults in the Levan-Fayette segment boundary area. Given the presence of many northwest-trending normal faults in this part of the western San Pitch Mountains (Mattox, 1987; Weiss and others, 2003), it seems likely that this fault took advantage of a pre-existing Tertiary structure.

A large part of the area of overlap between the Levan and Fayette segments (Flat Canyon graben of Felger, 1991, and Weiss and others, 2003) has been interpreted as an extensional structure modified by dissolution-induced collapse of the Arapien Shale (Felger, 1991). Alternatively, this area exhibits the structural characteristics of a relay ramp, where displacement is transferred between the overstepping ends of two normal fault sections having the same dip direction (see, for example, Larsen, 1988; Peacock and Sanderson, 1991). In particular, the presence of the fault in Chriss Canyon suggests a "stage 3" relay ramp (after Peacock and Sanderson, 1994) wherein faults cut across the relay ramp to connect the two overstepping fault sections (figure 10). Typically, relay ramps are interpreted as indicating that two fault sections are in the process of linking to become a single through-going fault; examples from Utah include overlapping sections of the Hurricane fault (Reber and others, 2001; Taylor and others, 2001; Lund and others, 2002; Amoroso and others, 2004) and Sevier fault (Reber and others, 2001). In the case of the Levan and Fayette segments, however, the Fayette part of the relay ramp and the Chriss Canyon connecting fault have been inactive since perhaps the middle Pleistocene. The spatial and temporal patterns of surface faulting (see discussion in Hylland, 2007b), as well as amounts of throw across the faults, indicate abandonment of the N strand of the Fayette segment and a westward shift in activity to the southern end of the Levan segment in late Quaternary time.

Southern Termination of the Wasatch Fault Zone

At the southern end of the Fayette segment, fault scarps on upper Quaternary deposits end east of the town of Fayette, near the Fayette Cemetery (SE1/4 section 19, T. 18 S., R. 1 E.). We observed no evidence of Quaternary faulting on-trend with the WFZ south of the town of Fayette. In southern Juab Valley, Schelling and others (2007) show the map trace of the WFZ curving to the southwest and terminating at the southern end of the valley. Whereas substantially decreased throw across the valley-margin fault and the distribution of Tertiary outcrops at the southern end of Juab Valley support this pattern of faulting, we follow Felger and others' (2007) inference of a concealed splay of the WFZ terminat-

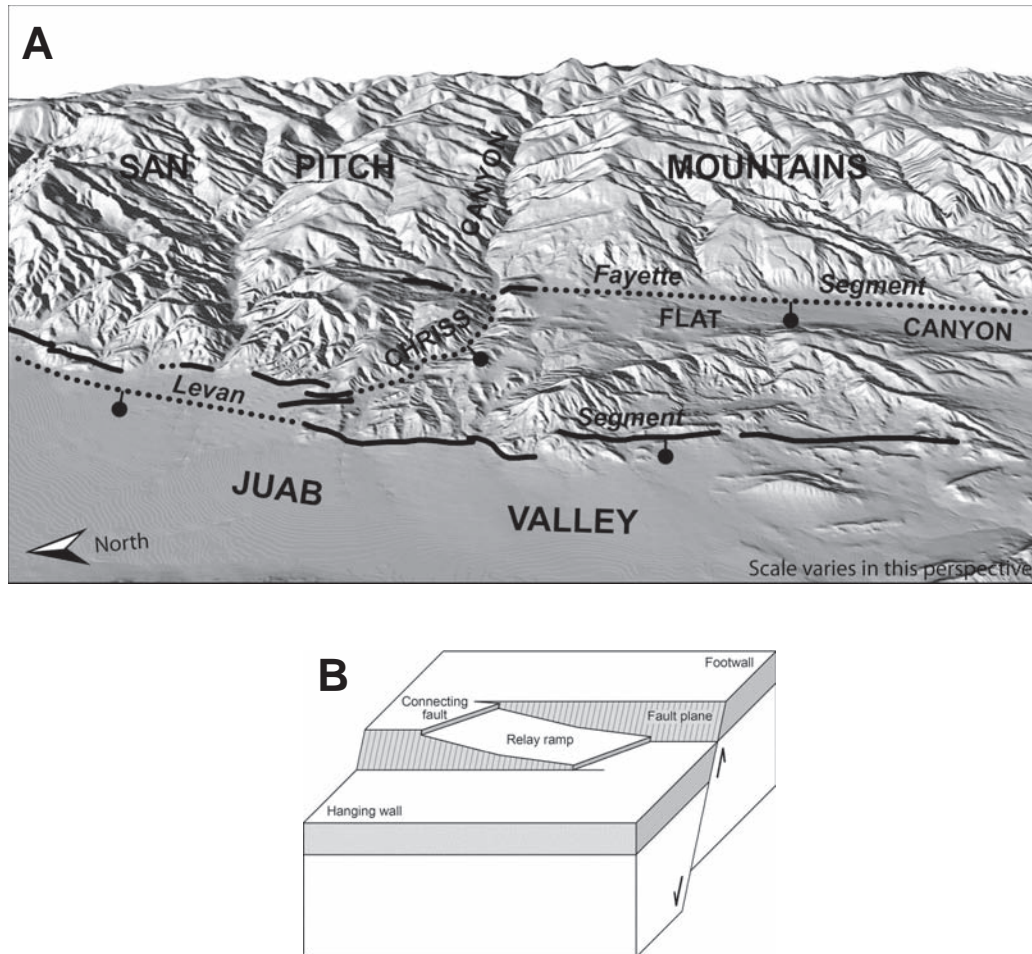


Figure 10. Map pattern of faulting in the Levan-Fayette segment boundary area suggests the presence of a relay ramp. (A) Oblique view (digital elevation model) of segment boundary area shows San Pitch Mountains in the footwall of the fault zone, Juab Valley in the hanging wall, and Flat Canyon occupying the eastern part of the relay ramp. Fault in Chriss Canyon is a connecting fault. Faults dotted where concealed, bar and ball on downthrown side. (B) Block diagram shows the main features of relay ramps (after Peacock and Sanderson, 1994).

ing at the southern end of Juab Valley. The southward continuation of late Quaternary, west-facing, normal-fault scarps along the western base of the San Pitch Mountains, as well as the apparent genetic association of the Levan and Fayette segments across the Flat Canyon relay ramp, suggest that the active WFZ continues into northern Sevier Valley and terminates near the town of Fayette as proposed by Schwartz and Coppersmith (1984) and Machette and others (1992).

Seismic-reflection and well data indicate the southern WFZ has a listric subsurface geometry that flattens at relatively shallow depth (~5 km) into low-angle structures—thrust faults that initially formed during the Cretaceous–early Tertiary Sevier orogeny and later reactivated as extensional structures. Although numerous regional cross sections in the area depict one or the other of the Levan and Fayette segments (see, for example, Standlee, 1982; Smith and Bruhn, 1984; Villien and Kligfield, 1986; DeCelles and Coogan, 2006; Schelling and others, 2007; Schelling and Vrona, 2007), the subsurface geometry of the two segments relative to each other is unclear. In their cross section near Chriss Canyon, Felger and others (2007) interpret the Levan and Fayette segments as splays off of a common reactivated

thrust fault. However, confirmation of this model would require increased resolution of subsurface data in the area.

Cline and Bartley (2002) have proposed that fault displacement at the southern end of the WFZ is transferred across the Sevier-Sanpete anticline (a Sevier-age, north-northeast-trending fold beneath the Sevier and Sanpete Valleys) to the Salina detachment, a low-angle, “rolling hinge”-style normal fault localized in the weak, evaporitic Arapien Shale. McKee and Arabasz (1982) and Arabasz and Julander (1986) noted that late Quaternary surface faulting south of the WFZ steps a few tens of kilometers to the west and southwest (i.e., to the Scipio, Pavant Range, Maple Grove, Japanese Valley, and Cal Valley faults [Hecker, 1993; Black and others, 2003]).

LATE QUATERNARY SLIP RATES

Accurate determination of late Quaternary slip rates for the Levan and Fayette segments is presently not possible. Paleoseismically determined earthquake timing information is available only for the MRE on the Levan segment (open seismic cycle), and no paleoseismically determined timing

information is available for the Fayette segment. However, we can use data from the Deep Creek exposure and Skinner Peaks trench to estimate a maximum Holocene vertical slip rate for the Levan segment, and geomorphic surface offset of upper to middle Pleistocene fan alluvium to estimate average long-term (geologic) vertical slip rates on both segments.

A maximum Holocene vertical slip rate for the Levan segment of about 0.3 mm/yr has been reported in compilations of data for Utah's Quaternary faults (Hecker, 1993; Black and others, 2001, 2003). This value is based on 1.8–2.0 m of NVTD for the MRE and the minimum elapsed time between the MRE and PE at Deep Creek. The time interval was calculated by subtracting Jackson's (1991) 1000 yr TL age for the MRE from Schwartz and Coppersmith's (1984) 7300 ¹⁴C yr B.P. age obtained on charcoal from near the bottom of the footwall exposure; given the presence of only a single wedge of scarp-derived colluvium in the hanging wall and the absence of any apparent unconformity in the footwall, the charcoal age probably provides a broad minimum limit on the timing of the PE (as suggested by Schwartz and Coppersmith [1984] and Jackson [1991]). However, the age obtained by Schwartz and Coppersmith is from detrital charcoal (the charcoal could be substantially older than the enclosing alluvium), has a large uncertainty (± 1000 yr) that was not considered in the slip-rate calculation, and was reported in radiocarbon years (the age needs to be calendar calibrated to be consistent with the TL age for the MRE). Using shortly after 1000 \pm 200 cal yr B.P. for MRE timing, sometime before 6000–10,600 cal yr B.P. for PE timing (the two-sigma calibration range that we determined for Schwartz and Coppersmith's radiocarbon age; appendix B), and 1.8 m NVTD (Jackson, 1991), we calculate a maximum vertical slip rate of 0.18–0.38 mm/yr for the Levan segment at Deep Creek (table 2, figure 11).

A maximum Holocene vertical slip rate for the Levan segment can also be calculated using data from the Skinner Peaks trench, although the results appear questionable (table 2). Based on projections of footwall surfaces across the fault relative to the base of the colluvial wedge on the hanging wall, Jackson (1991) calculated minimum and maximum NVTD for the MRE of 2.0 \pm 0.2 m and 2.8 \pm 0.2 m, respectively. Jackson's paleoearthquake timing estimates are 1000–1500 cal yr B.P. for the MRE, and sometime before

3100 \pm 300 to 3900 \pm 300 cal yr B.P. (reconverted to 4000 \pm 300 cal yr B.P. in this study; see appendix B) for the PE. Jackson's data, therefore, indicate a maximum vertical slip rate of 0.55–2.3 mm/yr for the Levan segment at Skinner Peaks (table 2, figure 11). Because the timing of the PE may have been considerably earlier than 2800–4300 cal yr B.P. (as suggested by the Schwartz and Coppersmith [1984] charcoal age at Deep Creek), these slip-rate estimates are probably too high. Also, the maximum NVTD value is anomalously large compared to single-event surface offsets derived from the scarp-profile data. Given that slip rates on the more active central segments of the Wasatch fault are in the 1–2 mm/yr range (Black and others, 2003; Lund, 2005), the high end of the range of estimated maximum slip rate for the clearly less-active Levan segment is likely not realistic.

In spite of the contextual uncertainty associated with the charcoal age obtained by Schwartz and Coppersmith (1984) at Deep Creek, we consider the slip rate calculated from the Deep Creek data to be more accurate than the rate calculated from the Skinner Peaks trench data. Therefore, our preferred maximum Holocene vertical slip rate for the Levan segment is 0.3 \pm 0.1 mm/yr. By way of comparison, the Utah Quaternary Fault Parameters Working Group, in their review of paleoseismic data for Utah faults, arrived at a consensus slip rate for the Levan segment of 0.1–0.6 mm/yr (Lund, 2005).

Average long-term (geologic) vertical slip rates on both the Levan and Fayette segments can be estimated from the geomorphic surface offset of upper to middle Pleistocene alluvial-fan deposits (100–250 ka; unit af4). Dividing net surface offset at various locations by these ages gives ranges of estimated long-term vertical slip rate of 0.02–0.05 mm/yr for the Levan segment and 0.01–0.03 mm/yr for the SE strand of the Fayette segment (table 3). However, using the minimum net surface offset of 14 m calculated for the large scarp at the north end of the SW strand of the Fayette segment results in a minimum long-term vertical slip rate of 0.06–0.1 mm/yr. This slip rate could be erroneously high due to our estimate of the age of the fan alluvium being too young, but the degree of calcic soil development and the geomorphology of the deposits support correlation with other upper to middle Pleistocene alluvial-fan deposits where the fault scarps are much lower. The higher slip rate on this part of the fault—near both the zone of overlap between the

Table 2. Maximum Holocene vertical slip rates for the Levan segment (see also figure 11).

| Site | NVTD ¹ (m) | MRE Timing (cal yr B.P.) | PE Timing (cal yr B.P.) | Inter-event Time (yr) | Slip Rate (mm/yr) |
|-------------------------|--------------------------|-----------------------------|----------------------------|--------------------------|----------------------|
| Deep Creek (stream cut) | 1.8 | < 800–1200 ² | > 6000–10,600 ³ | > 4800–9800 | < 0.18–0.38 |
| Skinner Peaks (trench) | 1.8–3.0 | 1000–1500 ¹ | > 2800–4300 ⁴ | > 1300–3300 | < 0.55–2.3 |

¹Jackson (1991).

²Timing from two-sigma uncertainty about median age of sample L-DC-RC1 (table B1).

³Timing from two-sigma uncertainty about median age of sample SC2 (table B1).

⁴Timing from one-sigma uncertainty about thermoluminescence age calculated for sample ITL-65 (Jackson, 1991, table 1) and two-sigma uncertainty about median age of sample Beta-24201 (table B1).

Abbreviations:

MRE, most recent event

NVTD, net vertical tectonic displacement

PE, penultimate event

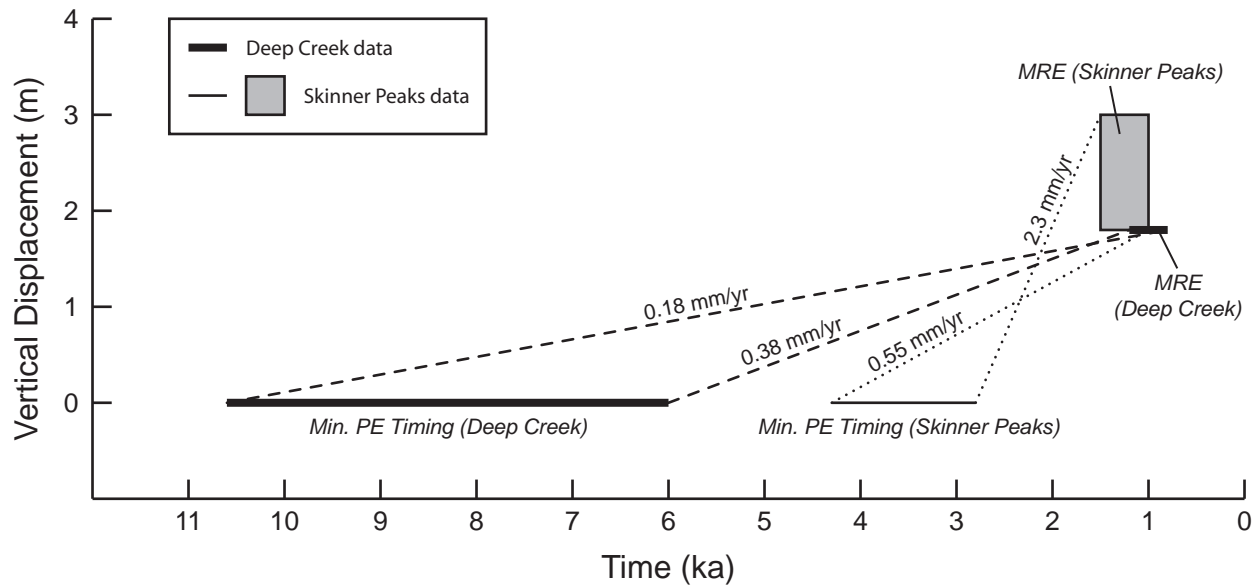


Figure 11. Graphical depiction of maximum Holocene vertical slip rates for the Levan segment, calculated using data from the Deep Creek natural exposure (Schwartz and Coppersmith, 1984; Jackson, 1991; this study) and Skinner Peaks trench (Jackson, 1991) (see also table 2). Horizontal lines and width of shaded box represent ranges of timing constraints for the most recent surface-faulting event (MRE; maximum time limit) and penultimate event (PE; minimum time limit). Height of shaded box represents Jackson's (1991) range of estimated displacement associated with the MRE. The ranges of the displacement and timing values yield maximum Holocene vertical slip rates of 0.18–0.38 mm/yr based on the Deep Creek data (dashed lines) and 0.55–2.3 mm/yr based on the Skinner Peaks data (dotted lines).

Table 3. Estimated middle to late Quaternary vertical slip rates for the Levan and Fayette segments.

| Site ¹ | S (m) | Deposit Age ² | Slip Rate (mm/yr) | Comments |
|---|-------|--------------------------|-------------------|--|
| Levan Segment: Spring Hollow, profile m64 | 4.8 | 100–250 ka | 0.019–0.048 | Correlative surfaces across fault |
| Fayette Segment: Hells Kitchen Canyon, profile F87.1 | ≥14 | 100–250 ka | > 0.056–0.14 | Hanging-wall surface younger than footwall surface, so rate is a minimum |
| Rough Canyon, profile F93 | 2.8 | 100–250 ka | 0.011–0.028 | Correlative surfaces across fault |
| Axhandle Canyon, profile m94 | 2.7 | 100–250 ka | 0.011–0.027 | Correlative surfaces across fault |
| Mellor Canyon, profile m99 | ≥3.2 | 100–250 ka | > 0.013–0.032 | Hanging-wall surface younger than footwall surface, so rate is a minimum |

¹Profile locations shown in appendix C.

²Deposit ages estimated from calcic soil development (see “Alluvial Deposits” discussion in text).

Abbreviation:

S, net geomorphic surface offset

Fayette and Levan segments and the bifurcation of the SW and SE strands of the Fayette segment—may result from Levan-segment surface-faulting earthquakes that rupture across the segment boundary onto the Fayette segment, additive slip from separate SW- and SE-strand ruptures that overlap on this part of the fault, or some combination of these two scenarios. Additionally, the higher slip rate may reflect a component of localized diapirism or dissolution-induced subsidence associated with subsurface evaporite beds in the Arapien Shale, and so may not be entirely the result of coseismic fault slip.

SUMMARY

The Levan and Fayette segments are the two southernmost segments of the Wasatch fault zone (WFZ). Quaternary deposits along the segments chiefly consist of piedmont-slope fan alluvium of middle Pleistocene to late Holocene age. Other Quaternary deposits present locally include unconsolidated to semiconsolidated fan alluvium of Quaternary-Tertiary age and fine-grained lacustrine deposits of late Pleistocene Lake Bonneville, as well as stream alluvium, landslide and debris-flow deposits, colluvium and talus, and eolian deposits.

The Levan and Fayette segments are clearly less active than the more central WFZ segments to the north, but nonetheless show evidence for recurrent late Quaternary surface faulting including Holocene events. The most recent event (MRE) on the Levan segment is well constrained by stratigraphic data and numerical ages as having occurred shortly after 1000 ± 200 cal yr B.P. Numerical ages indicate the penultimate event (PE) on the Levan segment occurred sometime prior to 2800–4300 cal yr B.P., and perhaps prior to 6000–10,600 cal yr B.P. Based on cross-cutting geologic relations and empirical analysis of scarp-profile data, MRE timing is different for the three strands of the Fayette segment: early or middle Pleistocene(?) for the N strand, latest Pleistocene for the SE strand, and Holocene for the SW strand. The timing of earlier surface-faulting earthquakes on the individual strands of the Fayette segment is unknown.

We place the northern boundary of the Levan segment in the area of Cedar Point, based on range-front geometry and a 5-km gap between late to middle Pleistocene fault scarps of the Levan segment and Holocene fault scarps of the Nephi segment. The boundary between the Levan and Fayette segments is a left-stepping area of overlap between the south end of the Levan segment on the west and the N strand of the Fayette segment on the east; structurally, the area of overlap appears to be a relay ramp. At the northern end of the area of overlap, a concealed, northwest-trending, down-to-the-south normal fault coincident with Chriss Canyon may be an oblique connecting structure between the Fayette and Levan

segments. North- and north-northeast-trending fault scarps and lineaments within the area of overlap are likely associated with structures that accommodate a left-stepping transfer of displacement between the two segments. The southern boundary of the Fayette segment is marked by the southward termination of late Quaternary fault scarps east of the town of Fayette.

Lack of well-constrained timing for the PE precludes accurate determination of a Holocene slip rate on the Levan segment. Using paleoseismic data from Deep Creek, we calculate a maximum vertical slip rate of 0.3 ± 0.1 mm/yr; data from the Skinner Peaks trench yield slip-rate estimates that are probably too high. Based on net geomorphic surface offset and estimated age of upper to middle Pleistocene fan alluvium near the middle of the segment, the middle to late Quaternary vertical slip rate for the Levan segment is 0.02–0.05 mm/yr.

The timing of surface-faulting paleoearthquakes on the Fayette segment is poorly constrained, so late Quaternary slip rates cannot be accurately determined. The estimated middle to late Quaternary vertical slip rate for the SE strand, determined from net geomorphic surface offset and estimated age of upper to middle Pleistocene fan alluvium, is 0.01–0.03 mm/yr. Using minimum net geomorphic surface offset calculated for the large scarp at the north end of the SW strand gives an estimated minimum long-term vertical slip rate of 0.06–0.1 mm/yr. The higher slip rate on this part of the fault may result from spillover of Levan-segment ruptures onto the Fayette segment, or additive slip from separate SW- and SE-strand Fayette-segment ruptures that overlap on this part of the fault, or some combination of these two scenarios. Additionally, the higher slip rate may reflect a component of aseismic deformation resulting from localized diapirism or dissolution-induced subsidence associated with subsurface evaporite beds in the Arapien Shale.

ACKNOWLEDGMENTS

This map was funded through a cooperative agreement between the Utah Geological Survey (UGS) and U.S. Geological Survey (USGS) (National Earthquake Hazards Reduction Program contract no. 03HQAG0008). Gary Christenson and Bill Lund (UGS) provided valuable advice and visited several field sites. Chris DuRoss (UGS) discussed his paleoseismic work on the Nephi segment and assisted with scarp profiling. Bob Biek, Don Clark, and Doug Sprinkel (UGS) shared their insights into the bedrock geology of the area. The map and report benefited from thoughtful reviews by Tom Judkins and Stephen Personius (USGS), and Gary Christenson, Chris DuRoss, Kimm Harty, and Robert Ressestar (UGS). Jim Parker and Lucas Shaw created several of the figures, and Lori Douglas did the cartography.

REFERENCES

- Amoroso, L., Pearthree, P.A., and Arrowsmith, J.R., 2004, Paleoseismology and neotectonics of the Shivwits section of the Hurricane fault, northwestern Arizona: *Bulletin of the Seismological Society of America*, v. 94, no. 5, p. 1919–1942.
- Anderson, J.J., and Rowley, P.D., 1975, Cenozoic stratigraphy of southwestern High Plateaus of Utah, *in* Anderson, J.J., Rowley, P.D., Fleck, R.J., and Nairn, A.E.M., Cenozoic geology of southwestern High Plateaus of Utah: Geological Society of America Special Paper 160, p. 1–51.
- Andrews, D.J., and Bucknam, R.C., 1987, Fitting degradation of shoreline scarps by a nonlinear diffusion model: *Journal of Geophysical Research*, v. 92, no. B12, p. 12,857–12,867.
- Arabasz, W.J., and Julander, D.R., 1986, Geometry of seismically active faults and crustal deformation within the Basin and Range–Colorado Plateau transition in Utah, *in* Mayer, L., editor, Extensional tectonics of the southwestern United States—a perspective on processes and kinematics: Geological Society of America Special Paper 208, p. 43–74.
- Auby, W.L., 1991, Provisional geologic map of the Levan quadrangle, Juab County, Utah: Utah Geological Survey Map 135, 13 p., 2 plates, scale 1:24,000.
- Baksi, A.K., Hsu, V., McWilliams, M.O., and Farrar, E., 1992, Ar-40/Ar-39 dating of the Brunhes-Matuyama geomagnetic field reversal: *Science*, v. 256, p. 356–357.
- Biek, R.F., 1991, Provisional geologic map of the Nephi quadrangle, Juab County, Utah: Utah Geological Survey Map 137, 21 p., 2 plates, scale 1:24,000.
- Biek, R.F., Solomon, B.J., Smith, T.W., and Keith, J.D., 2007, Geologic map of the Copperton quadrangle, Salt Lake County, Utah: Utah Geological Survey Map 219, 2 plates, scale 1:24,000.
- Birkeland, P.W., Machette, M.N., and Haller, K.M., 1991, Soils as a tool for applied Quaternary geology: Utah Geological and Mineral Survey Miscellaneous Publication 91-3, 63 p.
- Black, B.D., Hecker, S., Hylland, M.D., Christenson, G.E., and McDonald, G.N., 2003, Quaternary fault and fold database and map of Utah: Utah Geological Survey Map 193DM, scale 1:500,000, compact disk.
- Black, B.D., Hylland, M.D., McDonald, G.N., and Hecker, S., compilers, 2001, Fault number 2351i, Wasatch fault zone, Levan section, *in* Quaternary fault and fold database of the United States: Online, U.S. Geological Survey, <<http://earthquakes.usgs.gov/regional/qfaults>>, accessed 3/9/07.
- Bucknam, R.C., and Anderson, R.E., 1979, Estimation of fault-scarp ages from a scarp-height–slope-angle relationship: *Geology*, v. 7, p. 11–14.
- Callaghan, E., 1938, Preliminary report on the alunite deposits of the Marysvale region, Utah: U.S. Geological Survey Bulletin 886-D, p. 91–134.
- Christenson, G.E., and Purcell, C., 1985, Correlation and age of Quaternary alluvial-fan sequences, Basin and Range Province, southwestern United States, *in* Weide, D.L., editor, Soils and Quaternary geology of the southwestern United States: Geological Society of America Special Paper 203, p. 115–122.
- Clark, D.L., 1990, Provisional geologic map of the Juab quadrangle, Juab County, Utah: Utah Geological and Mineral Survey Map 132, 14 p., 2 plates, scale 1:24,000.
- Cline, E.J., and Bartley, J., 2002, Southern termination of the Wasatch fault localized by evaporite-cored Cretaceous anticline, Sevier Valley, UT [abs.]: Online, Geological Society of America, 2002 Denver Annual Meeting, <gsa.confex.com/gsa/2002AM/finalprogram/abstract_44233.htm>.
- Cluff, L.S., Brogan, G.E., and Glass, C.E., 1973, Wasatch fault, southern portion—earthquake fault investigation and evaluation—a guide to land use planning: Oakland, California, unpublished Woodward-Lundgren and Associates report, 79 p., 23 sheets, approximate scale 1:24,000.
- Crittenden, M.D., Jr., 1963, New data on the isostatic deformation of Lake Bonneville: U.S. Geological Survey Professional Paper 454-E, 31 p.
- Crone, A.J., editor, 1983, Paleoseismicity along the Wasatch Front and adjacent areas, central Utah, *in* Gurgel, K.D., editor, Geologic excursions in neotectonics and engineering geology in Utah, Guidebook—Part IV: Utah Geological and Mineral Survey Special Studies 62, p. 1–45.
- Currey, D.R., 1982, Lake Bonneville—selected features of relevance to neotectonic analysis: U.S. Geological Survey Open-File Report 82-1070, 30 p., 1 plate, scale 1:500,000.
- Currey, D.R., 1990, Quaternary paleolakes in the evolution of semidesert basins, with special emphasis on Lake Bonneville and the Great Basin, U.S.A.: *Palaeogeography, Palaeoclimatology, Palaeoecology*, v. 76, p. 189–214.
- DeCelles, P.G., and Coogan, J.C., 2006, Regional structure and kinematic history of the Sevier fold-and-thrust belt, central Utah: *Geological Society of America Bulletin*, v. 118, no. 7/8, p. 841–864 (doi: 10.1130/B25759.1).
- Felger, T.J., 1991, The geology of the Skinner Peaks quadrangle, Juab and Sanpete Counties, Utah: Duluth, University of Minnesota, M.S. thesis, 151 p., scale 1:24,000.
- Felger, T.J., Clark, D.L., and Hylland, M.D., 2007, Geologic map of the Skinner Peaks quadrangle, Juab and Sanpete Counties, Utah: Utah Geological Survey Map 223, 2 plates, scale 1:24,000, compact disk.
- Godsey, H.S., Currey, D.R., and Chan, M.A., 2005, New evidence for an extended occupation of the Provo shoreline and implications for regional climate change, Pleistocene Lake Bonneville, Utah, USA: *Quaternary Research*, v. 63, p. 212–223.
- Harty, K.M., Mulvey, W.E., and Machette, M.N., 1997, Surficial geologic map of the Nephi segment of the Wasatch fault zone, eastern Juab County, Utah: Utah Geological Survey Map 170, 14 p., scale 1:50,000.
- Hecker, S., 1993, Quaternary tectonics of Utah with emphasis on earthquake-hazard characterization: Utah Geological Survey Bulletin 127, 157 p., 2 plates.
- Hylland, M.D., 2007a, Surficial-geologic reconnaissance and scarp profiling on the Collinston and Clarkston Mountain segments of the Wasatch fault zone, Box Elder County, Utah—paleoseismic inferences, implications for adjacent segments, and issues for diffusion-equation scarp-age modeling—Paleoseismology of Utah, Volume 15: Utah Geological Survey Special Study 121, 18 p., compact disk.
- Hylland, M.D., 2007b, Spatial and temporal patterns of surface faulting on the Levan and Fayette segments of the Wasatch fault zone, central Utah, from surficial geologic mapping and scarp profile data, *in* Willis, G.C., Hylland, M.D., Clark, D.L., and Chidsey, T.C., Jr., editors, Central Utah—diverse geology of a dynamic landscape: Utah Geological Association Publication 36, p. 255–271.
- Jackson, M., 1991, The number and timing of Holocene paleoseismic events on the Nephi and Levan segments, Wasatch fault zone, Utah—Paleoseismology of Utah, Volume 3: Utah Geological Survey Special Study 78, 23 p.

- Keaton, J.R., 1987, Potential consequences of earthquake-induced regional tectonic deformation along the Wasatch Front, north-central Utah, *in* McCalpin, J., editor, Proceedings of the 23rd Symposium on Engineering Geology and Soils Engineering: Boise, Idaho Department of Transportation, p. 19–34.
- Keaton, J.R., Anderson, L.R., and Mathewson, C.C., 1991, Assessing debris flow hazards on alluvial fans in Davis County, Utah: Utah Geological Survey Contract Report 91-11, 167 p., 7 appendices.
- Larsen, P.H., 1988, Relay structures in a Lower Permian basement-involved extension system, East Greenland: *Journal of Structural Geology*, v. 10, p. 3–8.
- Lund, W.R., 2005, Consensus preferred recurrence-interval and vertical slip-rate estimates—review of Utah paleoseismic-trenching data by the Utah Quaternary Fault Parameters Working Group: Utah Geological Survey Bulletin 134, 109 p., compact disk.
- Lund, W.R., Taylor, W.J., Pearthree, P.A., Stenner, H., Amoroso, L., and Hurlow, H., 2002, Structural development and paleoseismicity of the Hurricane fault, southwestern Utah and northwestern Arizona, *in* Lund, W.R., editor, Field guide to geologic excursions in southwestern Utah and adjacent areas of Arizona and Nevada: U.S. Geological Survey Open-File Report 02-172, p. 1–84.
- Machette, M.N., 1982, Quaternary and Pliocene faults in the La Jencia and southern part of the Albuquerque-Belen basins, New Mexico—evidence of fault history from fault scarp morphology and Quaternary history, *in* Grambling, J.A., and Wells, S.G., editors, Albuquerque Country II: New Mexico Geological Society Guidebook, 33rd Field Conference, p. 161–169.
- Machette, M.N., 1985a, Calcic soils of the southwestern United States, *in* Weide, D.L., editor, Soils and Quaternary geology of the southwestern United States: Geological Society of America Special Paper 203, p. 1–21.
- Machette, M.N., 1985b, Late Cenozoic geology of the Beaver basin, southwestern Utah: *Brigham Young University Geology Studies*, v. 32, part 1, p. 19–37.
- Machette, M.N., 1992, Surficial geologic map of the Wasatch fault zone, eastern part of Utah Valley, Utah County and parts of Salt Lake and Juab Counties, Utah: U.S. Geological Survey Miscellaneous Field Investigations Series Map I-2095, 26 p., scale 1:50,000.
- Machette, M.N., Personius, S.F., and Nelson, A.R., 1992, Paleoseismology of the Wasatch fault zone—a summary of recent investigations, interpretations, and conclusions, *in* Gori, P.L., and Hays, W.W., editors, Assessment of regional earthquake hazards and risk along the Wasatch Front, Utah: U.S. Geological Survey Professional Paper 1500-A, 71 p.
- Machette, M.N., Personius, S.F., Nelson, A.R., Schwartz, D.P., and Lund, W.R., 1991, The Wasatch fault zone, Utah—segmentation and history of Holocene earthquakes: *Journal of Structural Geology*, v. 13, no. 2, p. 137–149.
- Mattox, S.R., 1987, Provisional geologic map of the Hells Kitchen Canyon SE quadrangle, Sanpete County, Utah: Utah Geological and Mineral Survey Map 98, 17 p., 2 plates, scale 1:24,000.
- Mattox, S.R., 1992, Provisional geologic map of the Gunnison quadrangle, Sanpete County, Utah: Utah Geological Survey Map 139, 11 p., 2 plates, scale 1:24,000.
- McCalpin, J.P., and Nishenko, S.P., 1996, Holocene paleoseismicity, temporal clustering, and probabilities of future large ($M > 7$) earthquakes on the Wasatch fault zone, Utah: *Journal of Geophysical Research*, v. 101, no. B3, p. 6233–6253.
- McKee, M.E., and Arabasz, W.J., 1982, Microearthquake studies across the Basin and Range–Colorado Plateau transition in central Utah, *in* Nielson, D.L., editor, Overthrust belt of Utah: Utah Geological Association Publication 10, p. 137–149.
- Nelson, A.R., and Personius, S.F., 1993, Surficial geologic map of the Weber segment, Wasatch fault zone, Weber and Davis Counties, Utah: U.S. Geological Survey Miscellaneous Field Investigations Series Map I-2199, 22 p., scale 1:50,000.
- Oviatt, C.G., 1987, Lake Bonneville stratigraphy at the Old River Bed, Utah: *American Journal of Science*, v. 287, p. 383–398.
- Oviatt, C.G., 1989, Quaternary geology of part of the Sevier Desert, Millard County, Utah: Utah Geological and Mineral Survey Special Studies 70, 41 p., 1 plate, scale 1:100,000.
- Oviatt, C.G., 1992, Quaternary geology of the Scipio Valley area, Millard and Juab Counties, Utah: Utah Geological Survey Special Study 79, 16 p., 1 plate, scale 1:62,500.
- Oviatt, C.G., Currey, D.R., and Sack, D., 1992, Radiocarbon chronology of Lake Bonneville, eastern Great Basin, USA: *Palaeogeography, Palaeoclimatology, Palaeoecology*, v. 99, p. 225–241.
- Oviatt, C.G., and Hintze, L.F., 2005, Interim geologic map of the Mills quadrangle, Juab County, Utah: Utah Geological Survey Open-File Report 445, 6 p., scale 1:24,000.
- Peacock, D.C.P., and Sanderson, D.J., 1991, Displacements, segment linkage and relay ramps in normal fault zones: *Journal of Structural Geology*, v. 13, p. 721–733.
- Peacock, D.C.P., and Sanderson, D.J., 1994, Geometry and development of relay ramps in normal fault systems: *American Association of Petroleum Geologists Bulletin*, v. 78, no. 2, p. 147–165.
- Personius, S.F., 1990, Surficial geologic map of the Brigham City segment and adjacent parts of the Weber and Collinston segments of the Wasatch fault zone, Box Elder and Weber Counties, Utah: U.S. Geological Survey Miscellaneous Field Investigations Series Map I-1979, scale 1:50,000.
- Personius, S.F., and Scott, W.E., 1992, Surficial geologic map of the Salt Lake City segment and parts of adjacent segments of the Wasatch fault zone, Davis, Salt Lake, and Utah Counties, Utah: U.S. Geological Survey Miscellaneous Field Investigations Series Map I-2106, scale 1:50,000.
- Petersen, D.H., 1997, Geologic map of the Hayes Canyon quadrangle, Sanpete County, Utah: Utah Geological Survey Miscellaneous Publication 97-3, 18 p., 2 plates, scale 1:24,000.
- Puseman, K., 2004, Examination of bulk soil and detrital charcoal for radiocarbon datable material from the Wasatch fault zone, Levan segment, near Skinner Peaks, Utah: Golden, Colorado, unpublished Paleo Research Institute Technical Report 04-59, prepared for the Utah Geological Survey, 6 p.
- Reber, S., Taylor, W.J., Stewart, M., and Schiefelbein, I.M., 2001, Linkage and reactivation along the northern Hurricane and Sevier faults, southwestern Utah, *in* Erskine, M.C., Faulds, J.E., Bartley, J.M., and Rowley, P.D., editors, The geologic transition, High Plateaus to Great Basin—a symposium and field guide—The Mackin Volume: Utah Geological Association Publication 30 and Pacific Section American Association of Petroleum Geologists Publication GB78, p. 379–400.

- Reimer, P.J., Baillie, M.G.L., Bard, E., Bayliss, A., Beck, J.W., Bertrand, C.J.H., Blackwell, P.G., Buck, C.E., Burr, G.S., Cutler, K.B., Damon, P.E., Edwards, R.L., Fairbanks, R.G., Friedrich, M., Guilderson, T.P., Hogg, A.G., Hughen, K.A., Kromer, B., McCormac, G., Manning, S., Ramsey, C.B., Reimer, R.W., Remmele, S., Southon, J.R., Stuiver, M., Talamo, S., Taylor, F.W., van der Plicht, J., and Weyhenmeyer, C.E., 2004, IntCal04 terrestrial radiocarbon age calibration, 0–26 cal kyr BP: *Radiocarbon*, v. 46, no. 3, p. 1029–1058.
- Schelling, D.D., Strickland, D., Johnson, K., and Vrona, J., 2007, Structural geology of the central Utah thrust belt, *in* Willis, G.C., Hylland, M.D., Clark, D.L., and Chidsey, T.C., Jr., editors, *Central Utah—diverse geology of a dynamic landscape*: Utah Geological Association Publication 36, p. 1–29.
- Schelling, D.D., and Vrona, J., 2007, Structural geology of the central Utah thrust belt—a geological field trip road log, *in* Willis, G.C., Hylland, M.D., Clark, D.L., and Chidsey, T.C., Jr., editors, *Central Utah—diverse geology of a dynamic landscape*: Utah Geological Association Publication 36, p. 483–518.
- Schwartz, D.P., and Coppersmith, K.J., 1984, Fault behavior and characteristic earthquakes—examples from the Wasatch and San Andreas fault zones: *Journal of Geophysical Research*, v. 89, no. B7, p. 5681–5698.
- Smith, R.B., and Bruhn, R.L., 1984, Intraplate extensional tectonics of the eastern Basin-Range—*inferences on structural style from seismic reflection data, regional tectonics, and thermal-mechanical models of brittle-ductile deformation*: *Journal of Geophysical Research*, v. 89, no. B7, p. 5733–5762.
- Spieker, E.M., 1949, The transition between the Colorado Plateaus and the Great Basin in central Utah: *Utah Geological Society, Guidebook to the Geology of Utah*, no. 4, 106 p., 1 plate.
- Standlee, L.A., 1982, Structure and stratigraphy of Jurassic rocks in central Utah—their influence on tectonic development of the Cordilleran foreland thrust belt, *in* Powers, R.B., editor, *Geologic studies of the Cordilleran thrust belt, Volume I*: Denver, Rocky Mountain Association of Geologists, p. 357–382.
- Stuiver, M., and Reimer, P.J., 1986, A computer program for radiocarbon age calibration: *Radiocarbon*, v. 28, p. 1022–1030.
- Swenson, J.L., Jr., Beckstrand, D., Erickson, D.T., McKinley, C., Shiozaki, J.J., and Tew, R., 1981, Soil survey of Sanpete Valley area, Utah—parts of Utah and Sanpete Counties: U.S. Department of Agriculture, Soil Conservation Service, and U.S. Department of the Interior, Bureau of Land Management, 179 p., 67 sheets, scale 1:24,000.
- Taylor, W.J., Stewart, M.E., and Orndorff, R.L., 2001, Fault segmentation and linkage—examples from the Hurricane fault, southwestern U.S.A., *in* Erskine, M.C., Faulds, J.E., Bartley, J.M., and Rowley, P.D., editors, *The geologic transition, High Plateaus to Great Basin—a symposium and field guide—The Mackin Volume*: Utah Geological Association Publication 30 and Pacific Section American Association of Petroleum Geologists Publication GB78, p. 113–126.
- Trickler, D.L., and Hall, D.T., 1984, Soil survey of Fairfield-Nephi area, Utah—parts of Juab, Sanpete, and Utah Counties: U.S. Department of Agriculture, Soil Conservation Service, 361 p., 130 sheets, scale 1:24,000.
- Villien, A., and Kligfield, R.M., 1986, Thrusting and synorogenic sedimentation in central Utah, *in* Peterson, J.A., editor, *Paleotectonics and sedimentation in the Rocky Mountain region, United States*: American Association of Petroleum Geologists Memoir 41, p. 281–307.
- Wallace, R.E., 1977, Profiles and ages of young fault scarps, north-central Nevada: *Geological Society of America Bulletin*, v. 88, no. 9, p. 1267–1281.
- Weiss, M.P., McDermott, J.G., Sprinkel, D.A., Banks, R.L., and Biek, R.F., 2003, Geologic map of the Chriss Canyon quadrangle, Juab and Sanpete Counties, Utah: *Utah Geological Survey Map 185*, 26 p., 2 plates, scale 1:24,000.
- Western Regional Climate Center, undated, Utah climate summaries: Online, <<http://www.wrcc.dri.edu/summary/climmut.html>>, accessed 2/9/05.
- Willis, G.C., 1988, Geologic map of the Aurora quadrangle, Sevier County, Utah: *Utah Geological and Mineral Survey Map 112*, 21 p., scale 1:24,000.
- Willis, G.C., 1991, Geologic map of the Redmond Canyon quadrangle, Sanpete and Sevier Counties, Utah: *Utah Geological Survey Map 138*, 17 p., scale 1:24,000.
- Witkind, I.J., Weiss, M.P., and Brown, T.L., 1987, Geologic map of the Manti 30' x 60' quadrangle, Carbon, Emery, Juab, Sanpete, and Sevier Counties, Utah: U.S. Geological Survey Miscellaneous Investigations Series Map I-1631, scale 1:100,000.

APPENDIX A

DESCRIPTION OF MAP UNITS

Map-unit descriptions are organized by genesis (mode of formation) and age (young to old). Quaternary geologic map units were differentiated using relative-age criteria such as stratigraphic position, geomorphic expression, and soil-profile development. To the extent possible, age categories are based on climatic cycles (i.e., correlation with lacustrine sediment deposited during pluvial lake cycles in the Bonneville basin). However, the limited duration and extent of Lake Bonneville in the map area (see "Lacustrine History and Related Deposits") precludes the widespread use of this approach for this map. Map-unit symbols generally follow the convention used on the previously published surficial geologic maps of the Wasatch fault zone. Unit thicknesses are generally rounded to the nearest 5 m.

Quaternary Deposits

Lacustrine Deposits

Lacustrine deposits accumulated in a shallow arm of late Pleistocene Lake Bonneville, which occupied the southernmost part of Juab Valley and northern part of Sevier Valley for a period of about 3000 years leading up to the Bonneville Flood at 16.8 ka. The fine-grained clastic sediment was likely deposited in an underflow-fan type of deltaic environment (after Oviatt, 1987, 1989). Because of the valley-floor elevations in the map area relative to major lake levels, only deposits associated with the Bonneville (transgressive) phase and shoreline of the Bonneville lake cycle are present.

- lbs **Lacustrine sand (upper Pleistocene)** – Interbedded, well-sorted fine sand, silt, and clay; thin to thick bedded. Deposited in a nearshore/beach environment during the Bonneville lake-cycle highstand. Locally reworked by wind into small dunes now stabilized by vegetation. Exposed thickness about 2 m.
- lbm **Lacustrine silt and clay (upper Pleistocene)** – Interbedded silt and clay with minor fine sand; thin to thick bedded; contains small conspiral gastropod shells and bivalve shells as much as 5 cm across. Ground surface locally displays polygonal pattern of shrinkage cracks, indicating presence of expansive clay. Near the wave-cut Bonneville shoreline on the west side of the Painted Rocks, unit locally contains abundant, angular clasts of tuff eroded from the adjacent rock slope. Exposed thickness as much as 25 m in bluffs along the margins of the Sevier River flood plain.
- lbmg **Lacustrine silt and clay with gravel (upper Pleistocene)** – Interbedded silt and clay with minor fine sand, and thin beds of pebble gravel in the upper part of the unit; clasts are subangular to rounded. Gravel probably deposited locally by tributary streams in a shoreline environment during lake-level oscillations associated with the Bonneville lake-cycle highstand.

Stream Alluvium

- al1 **Stream alluvium, unit 1 (upper Holocene)** – Gravel, sand, and silt with lesser amounts of clay, and scattered cobbles and boulders; clasts well rounded to subangular; generally stratified. Deposited in modern stream channels and on adjacent flood plains; locally grades downslope into upper Holocene alluvial-fan deposits (unit af1). May include small alluvial fans, debris-flow deposits, and minor amounts of locally derived colluvium along steep stream embankments. Exposed thickness <5 m.
- alf **Alluvium of Sevier River flood plain (Holocene)** – Mostly clay with silt and fine sand; comprises a mixture of fine-grained fluvial sediment and lacustrine deposits of the Bonneville highstand that were subsequently reworked by lateral channel migration. Episodic modern lacustrine deposition occurs below elevation 5014 ft when impounded water of Sevier Bridge Reservoir is present. Thickness unknown.
- al2 **Stream alluvium, unit 2 (middle Holocene to uppermost Pleistocene)** – Gravel, sand, and silt with lesser amounts of clay, and scattered cobbles and boulders; clasts well rounded to subangular; generally stratified. May include small alluvial fans, debris-flow deposits, and minor locally derived colluvium along steep stream embankments. Generally forms terraces less than 5 m above modern streams and has soils with stage I–II carbonate morphology; locally grades downslope into intermediate-level alluvial-fan deposits (unit af2). Although physical correlation with deposits of the Bonneville lake cycle cannot be established, the relatively low terrace heights and weak soil-profile development suggest post-Bonneville deposition. Exposed thickness <5 m.
- aly **Younger stream alluvium, undivided (Holocene to upper Pleistocene)** – Undivided stream alluvium (units al1 and al2) that postdates regression of Lake Bonneville, as well as stream alluvium probably deposited during the Bonneville lake cycle; physical correlation with deposits of the Bonneville lake cycle cannot be established. Thickness variable, generally <15 m.

- alo **Older stream alluvium, undivided (upper to middle Pleistocene)** – Stream alluvium underlying abandoned surfaces in the area of Old Pinery Canyon and Gardners Fork; consists of gravel, sand, and silt with cobbles and minor clay, locally bouldery; clasts well rounded to subangular; generally stratified. May include small alluvial fans, debris-flow deposits, and minor locally derived colluvium along steep stream embankments. Deposits generally form broad, incised surfaces as much as 40 m above modern streams and have soils with stage II–III carbonate morphology. Exposed thickness generally 10–40 m.
- ap **Pediment-mantle alluvium (middle? to lower? Pleistocene)** – Stream and fan alluvium that mantles a relatively planar, dissected surface of erosion formed on Quaternary-Tertiary basin-fill and alluvial-fan deposits, and possibly Tertiary bedrock; consists of poorly sorted gravel, sand, and silt with lesser amounts of clay, and scattered cobbles and boulders. Deposits are as much as 30 m above adjacent drainages. Exposed thickness <15 m.
- ac **Alluvium and colluvium, undivided (Holocene to upper Pleistocene)** – Primarily stream and fan alluvium with subordinate hillslope colluvium; may also locally include eolian sediment. Deposited in shallow drainages associated with intermittent streams, and in small, shallow basins. Thickness variable, but generally <5 m.
- ab **Undifferentiated basin-fill alluvium (Holocene and Pleistocene)** – Variable mixtures of gravel, sand, silt, and clay; clasts well rounded to subangular; generally stratified. Deposited by intermittent streams in southern Juab Valley and northern Sevier Valley where alluvial fans are poorly developed or absent. Highly variable clast composition and gradation, soil development, and thickness.

Fan Alluvium

- af1 **Fan alluvium, unit 1 (upper Holocene)** – Pebble and cobble gravel, locally bouldery, in a matrix of sand, silt, and minor clay; clasts angular to subrounded. Deposited by intermittent streams, debris flows, and debris floods graded to modern stream level. Deposits form discrete fans, typically with original bar and swale topography. Local soils have weak stage I carbonate morphology. Exposed thickness <5 m.
- af2 **Fan alluvium, unit 2 (middle Holocene to uppermost Pleistocene)** – Pebble and cobble gravel, locally bouldery, in a matrix of sand, silt, and minor clay; clasts angular to well rounded. Deposited by intermittent streams, debris flows, and debris floods graded to or slightly above modern stream level. Locally preserved as intermediate-level remnants incised by modern streams; soils have stage I–II carbonate morphology. Exposed thickness <5 m.
- afy **Younger fan alluvium, undivided (Holocene to uppermost Pleistocene)** – Undivided fan alluvium (units af1 and af2) that postdates regression of Lake Bonneville. Thickness unknown.
- afb **Fan alluvium related to Bonneville phase of the Bonneville lake cycle (upper Pleistocene)** – Pebble and cobble gravel, locally bouldery, in a matrix of sand, silt, and minor clay; clasts angular to well rounded. Deposited by intermittent streams, debris flows, and debris floods graded approximately to the upper surface of lacustrine deposits of the Bonneville highstand. Exposed thickness <5 m.
- afc **Coalesced fan alluvium (Holocene to upper? Pleistocene)** – Pebble and cobble gravel, locally bouldery, in a matrix of sand, silt, and minor clay; clasts subangular to well rounded. Overall, deposits become finer grained away from valley margins. Deposited by perennial and intermittent streams, debris flows, and debris floods graded to or slightly above modern stream level; locally includes a significant component of eolian silt. Deposits form large, low-gradient fans that cover much of the floor of Juab Valley, Flat Canyon, and the eastern part of Sevier Valley. Locally includes deposits of units af1 and cd1 too small to map separately. Thickness variable; maximum thickness unknown.
- af4 **Fan alluvium, unit 4 (upper to middle Pleistocene; pre-Bonneville lake cycle)** – Pebble and cobble gravel, locally bouldery, in a matrix of sand, silt, and minor clay; clasts subangular to well rounded. Preserved as relatively high, isolated remnants that generally lack fan morphology; soils have stage II–IV carbonate morphology. Deposits west of the Sevier River are locally overlain by, and therefore predate, lacustrine deposits of the Bonneville highstand. Exposed thickness <20 m.
- afo **Older fan alluvium, undivided (upper to middle Pleistocene; pre-Bonneville lake cycle)** – Undivided fan alluvium (unit af4 and possibly older deposits) that predates the Bonneville lake cycle. Mapped where high-level alluvial-fan deposits are poorly exposed or lack distinct geomorphic expression. Locally includes exposures of unit QTaf too small to map separately. Thickness unknown.

Eolian Deposits

- es **Eolian sand (Holocene to uppermost Pleistocene)** – Well-sorted fine-grained sand; structureless and unconsolidated. Exposed thickness <3 m.

Colluvial and Mass-Movement Deposits

- cd1 **Debris-flow deposits, unit 1 (upper Holocene)** – Primarily matrix-supported pebble and cobble gravel, locally bouldery; clasts angular; matrix consists of sand, silt, and clay; includes lesser beds of clast-supported (alluvial) gravel. Commonly has relatively young-looking levees and channels. Generally deposited on surface of Holocene alluvial fans (units afy and af1); deposits too small to map separately are included in those units. Exposed thickness <5 m.
- chs **Hillslope colluvium (Holocene to upper Pleistocene)** – Pebble, cobble, and boulder gravel in a matrix of sand, silt, and clay; unsorted and poorly stratified. Deposited by slope-wash and mass-wasting processes on relatively steep slopes. Exposed thickness <5 m.
- cfs **Fault-scarp colluvium (Holocene to upper Pleistocene)** – Gravel, cobbles, sand, and minor silt and clay; unsorted to poorly sorted. Present along most fault scarps, but mapped only on the lower part of large (>20 m high) scarps where the colluvium has accumulated in a wedge to a thickness of about 2 m on the downdropped side of the fault.
- crf **Rock-fall and talus deposits (Holocene to upper Pleistocene)** – Clast-supported pebble, cobble, and boulder gravel; unsorted and unstratified; angular to subangular. Typically forms cones and sheets at or near the angle of repose (~35°). Exposed thickness <5 m.
- clsy **Younger landslide deposits (Holocene to upper Pleistocene)** – Unsorted, unstratified material that has moved downslope by rotational or translational gravity-induced slip. Relatively fresh main scarps and hummocky topography indicate recency of initial or reactivated movement. Thickness highly variable.
- clso **Older landslide deposits (Pleistocene)** – Unsorted, unstratified material that has moved downslope by rotational or translational gravity-induced slip. Main scarps and landslide surfaces are dissected and landslide morphology is subdued, indicating relatively old age of initiation of movement. May include younger landslides (unit clsy) too small to map separately. Thickness highly variable.
- ca **Colluvium and alluvium, undivided (Holocene to upper Pleistocene)** – Primarily hillslope colluvium with subordinate stream and fan alluvium, and small landslide deposits. Thickness variable.

Artificial Deposits

- fd **Artificial fill and associated disturbed ground (historical)** – Primarily locally derived surficial material placed or disturbed during construction or mining activities. Includes embankments, pits, waste rock piles, and landfills. Present throughout the map area, but only the largest areas are shown.

Quaternary-Tertiary Deposits

- QTaf **Quaternary-Tertiary alluvial-fan deposits (middle Pleistocene to Miocene?)** – Unconsolidated to semiconsolidated, poorly sorted fan alluvium generally preserved in isolated remnants as much as 150 m above modern stream level; clasts include cobbles and boulders of quartzite, sandstone, limestone, and volcanic rocks. Fan surfaces locally strewn with carbonate rubble weathered from underlying calcic paleosol horizons. As much as 150 m thick.
- QTab **Quaternary-Tertiary basin-fill deposits (lower? Pleistocene to Miocene?)** – Weakly to moderately consolidated alluvial deposits of clay, silt, and sand with interbedded pebble to cobble gravel; poorly to relatively well stratified. Gravel is clast supported, and clasts are moderately to well rounded and well sorted. Local exposures on the horst block of the Dover fault zone reveal a calcic paleosol with stage IV (laminar) carbonate morphology. Thickness unknown.

Bedrock

Bedrock units are not shown in detail on the map. For more information on the bedrock geology of the area, consult the geologic quadrangle maps shown on figure 3 in the report. Bedrock areas may include thin, unmapped deposits of hillslope colluvium.

- Ti **Tertiary intrusive rocks (Miocene)** – Monzonite porphyry, leucomonzonite, and syenite of the Levan monzonite suite of Auby (1991).
- Tv **Tertiary volcanoclastic rocks (Oligocene to Eocene)** – Conglomerate, sandstone, and tuff of the Golden Ranch Formation and formation of Painted Rocks (Felger and others, 2007).
- Ts **Tertiary sedimentary rocks (Eocene to Upper Cretaceous?)** – Includes the following bedrock formations: Eocene Crazy Hollow Formation (cherty sandstone), Eocene Green River Formation (limestone, sandstone, and mudstone),

Eocene Colton Formation (mudstone, limestone, and sandstone), Eocene-Paleocene Flagstaff Limestone (limestone and sandstone), and Eocene–Upper Cretaceous(?) North Horn Formation (conglomerate and sandstone).

Mz Mesozoic sedimentary rocks (Upper Cretaceous and Middle Jurassic) – Conglomerate and pebbly sandstone of the Upper Cretaceous Indianola Group, and shaly limestone, sandstone, siltstone, mudstone, and gypsum of the Middle Jurassic Arapien Shale and Twin Creek Limestone.

APPENDIX B

RADIOCARBON ANALYSES AND CALENDAR CALIBRATION

We obtained three samples of organic material from fan alluvium along the Levan segment for radiocarbon dating to help constrain paleoearthquake timing. Our attempts to recover organic material from along the Fayette segment for radiocarbon dating were unsuccessful. We converted the radiocarbon ages to calendar-calibrated ages using the CALIB (version 5.0.1) radiocarbon calibration program (after Stuiver and Reimer, 1986), which incorporates the INTCAL04 (Northern Hemisphere, atmospheric) calibration dataset (Reimer and others, 2004). We also used CALIB to convert radiocarbon ages obtained by others during previous studies to calendar-calibrated ages to be consistent with reported thermoluminescence ages and modern Wasatch fault zone paleoearthquake chronologies.

The radiocarbon ages are reported in years before present (A.D. 1950). The calendar-calibrated ages that we cite in the text represent the midpoint of the two-sigma (95% probability) calibration ranges; these “median ages” and their associated errors are rounded to the nearest century to account for both epistemic (incomplete or imperfect knowledge of system processes) and aleatory (inherent variation in the system) uncertainties. Table B1 summarizes the radiocarbon and calendar-calibrated ages.

Samples Obtained During This Study

We obtained three samples (L-DC-RC1, L-SP-RC1, and L-SP-RC2) of organic material from fan alluvium along the Levan segment (see plate 1 for sample locations). The samples were analyzed by Beta Analytic, Inc. of Miami, Florida. Sample L-DC-RC1 (bulk soil) was analyzed using conventional radiometric techniques, and samples L-SP-RC1 and L-SP-RC2 (detrital charcoal) were analyzed using accelerator mass spectrometry (AMS). Sample pretreatment consisted of acid (HCl) washes for conventional analysis, and acid and alkali (NaOH) washes for AMS analysis. The radiocarbon ages were $\delta^{13}\text{C}$ corrected by the laboratory.

Sample L-DC-RC1

We obtained sample L-DC-RC1 from the natural exposure of the Wasatch fault at Deep Creek (section 18, T. 15 S., R. 1 E., SLBLM). We sampled the uppermost 5 cm of the organic A horizon paleosol directly overlain by scarp-derived colluvium in the hanging wall of the fault. The resulting apparent mean residence time (AMRT) age of 1200 ± 80 ^{14}C yr B.P. provides a close maximum limit on the timing of scarp formation. The radiocarbon age calendar calibrates to 970–1280 cal yr B.P. (two sigma). Because we sampled a thin interval, we apply a relatively small mean residence time correction of 100 years for the age of carbon at the time of burial (following the approach described by Machette and others, 1992, and McCalpin and Nishenko, 1996) and subtract this from the calendar-calibrated age; this produces the calibration range and median age given in table B1.

Samples L-SP-RC1 and L-SP-RC2

We obtained samples L-SP-RC1 and L-SP-RC2 from the side of a small gully incised into alluvial-fan deposits near Skinner Peaks (NW1/4 section 15, T. 16 S., R. 1 W., SLBLM). The sample site (figure B1) is on the footwall of the Wasatch fault, about 25 m southeast of (upgradient from) the scarp (vicinity of scarp profiles m82 and m83; see table C2) (see plate 1 for sample location). Sample L-SP-RC1 was obtained from the uppermost 3 cm of a weakly organic A horizon paleosol at a depth of about 1.0 m below the ground surface. Very small (≤ 0.002 g) charcoal fragments were mechanically separated from the bulk-soil sample and identified as saltbush (*Atriplex*) and juniper (*Juniperus*) by Paleo Research Institute of Golden, Colorado (Puseman, 2004). Because of their very small size, the fragments were recombined for AMS analysis. Sample L-SP-RC2 consisted of a single fragment of detrital charcoal (*Juniperus*; Puseman, 2004) obtained from about 15 cm below the organic paleosol.

Because the sampled charcoal is detrital and had existed for some unknown amount of time prior to being incorporated into the fan alluvium, the radiocarbon ages provide a maximum limit on the age of the deposit. Together, the two samples produced stratigraphically consistent radiocarbon ages that document late Holocene alluvial-fan deposition. However, whereas the radiocarbon ages provide insight into the age of the faulted fan alluvium, they do not necessarily constrain the timing of scarp formation because a clear stratigraphic and structural relation between the sampled deposits and the fault is lacking.

Calendar Calibration of Previous Radiocarbon Ages

Three radiocarbon ages of charcoal collected from faulted fan alluvium along the Levan segment were published by others following previous reconnaissance studies (Crone, 1983; Schwartz and Coppersmith, 1984). The reported ages had not been calendar calibrated, so to facilitate their use in the context of modern paleoearthquake chronologies, we converted them to calendar-calibrated ages as part of this study. Also, in his paleoseismic trenching study near Skinner Peaks, Jackson (1991) calendar calibrated his radiocarbon ages of organic material collected from the trench, but we reconverted them in this study to make use of the more recent INTCAL04 calibration dataset.

Table B1. Radiocarbon dating and calendar calibrations.

| Sample/Lab ID | Location/ UTM ¹ | Sample Description | Radiocarbon Age (¹⁴ C yr B.P.) | Calendar-Calibrated Age ² (2 σ calibration range/median age) (cal yr B.P.) | Source of Original Data |
|---------------------------|---|---|--|--|--|
| L-DC-RC1 (Beta-184780) | Deep Creek (E04 25990 N43 73310) | Bulk soil, upper 5 cm of A horizon buried by scarp-derived colluvium (hanging wall) | 1200 \pm 80 (radiometric) | 870–1180 ³ (1000 \pm 200) | This study |
| L-SP-RC1 (Beta-195375) | Skinner Peaks (E04 21103 N43 63711) | Detrital charcoal separ- ated from buried A hori- zon paleosol in fan allu- vium (footwall); sample depth 1 m | 1630 \pm 40 (AMS) | 1410–1610 (1500 \pm 100) | This study |
| L-SP-RC2 (Beta-194451) | Skinner Peaks (E04 21103 N43 63711) | Detrital charcoal in fan alluvium, beneath buried A horizon paleosol (foot- wall); sample depth 1.15 m | 3230 \pm 50 (AMS) | 3360–3570 (3500 \pm 200) ⁴ | This study |
| Beta-24200 | Skinner Peaks trench | Charcoal from buried burn horizon in fan alluvium (footwall) | 1850 \pm 70 (radiometric) | 1610–1940 (1800 \pm 200) | Jackson (1991) |
| Beta-24201 | Skinner Peaks trench | Concentrated charcoal from buried A horizon (hanging wall) | 3720 \pm 90 (radiometric) | 3740–4200 ³ (4000 \pm 300) ⁴ | Jackson (1991) |
| C1 | Pigeon Creek | Detrital charcoal in fan alluvium | 2100 \pm 300 (AMS) | 1410–2760 (2100 \pm 700) | Crone (1983) |
| SC1 | Pigeon Creek | Detrital charcoal in fan alluvium | 1750 \pm 350 (AMS) | 950–2490 (1700 \pm 800) | Crone (1983), Schwartz and Coppersmith (1984) |
| SC2 | Deep Creek | Detrital charcoal in fan alluvium, low in footwall exposure | 7300 \pm 1000 (AMS) | 5980–10,590 (8300 \pm 2300) | Schwartz and Coppersmith (1984) |

¹All samples are from the Levan segment.

²Two-sigma (95% probability) calibration ranges rounded to nearest decade; median ages and uncertainties rounded to nearest century.

³Calibration ranges reflect subtraction of 100-year mean residence time correction.

⁴Uncertainty was increased by 100 years to account for the effects of rounding relative to the calibration range.

Abbreviations:

AMS, accelerator mass spectrometry

UTM, Universal Transverse Mercator (1983 North American datum)

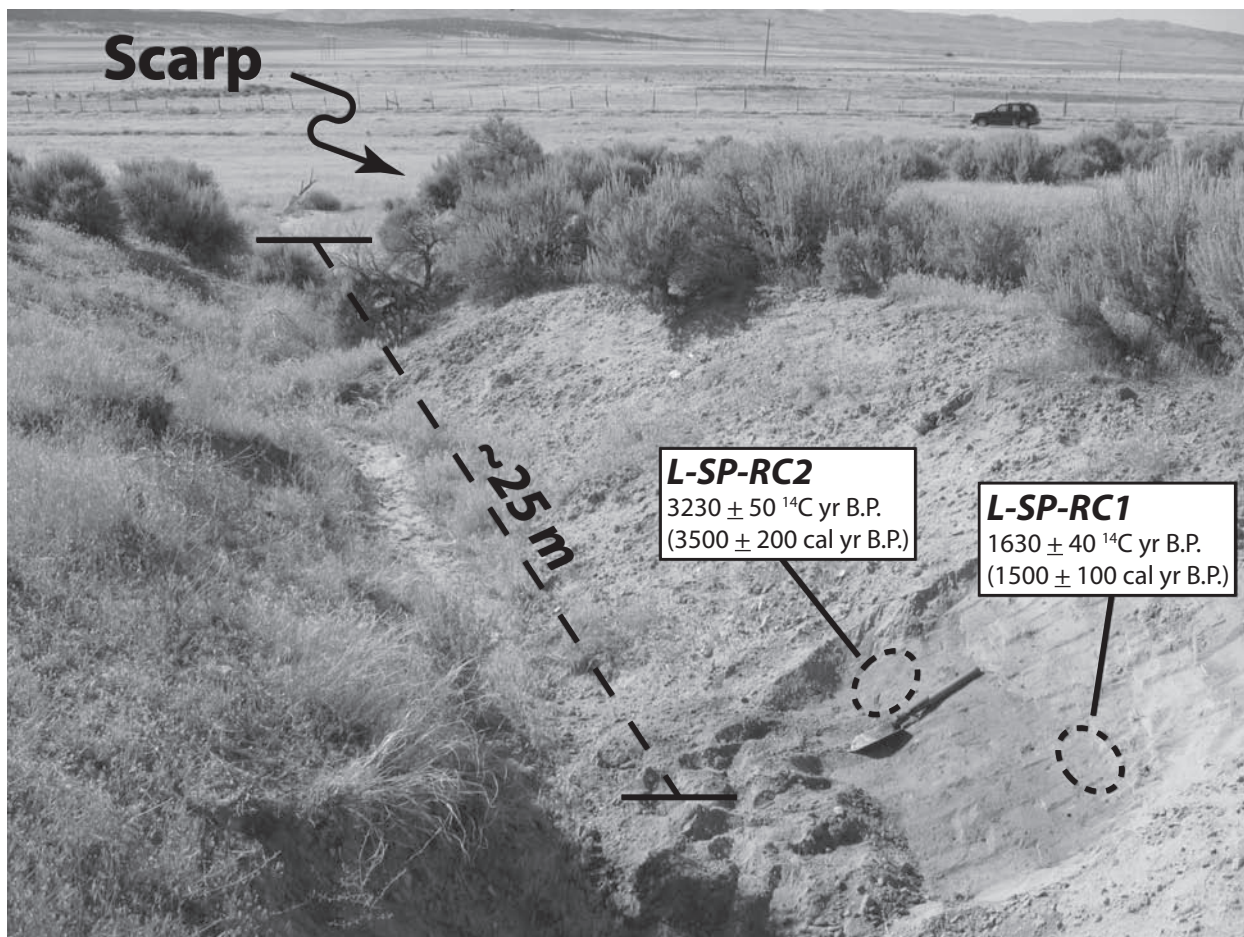


Figure B1. Site of samples L-SP-RC1 and L-SP-RC2, collected from faulted fan alluvium along the Levan segment near Skinner Peaks for radiocarbon dating (view looking northwest). Folding shovel (0.57 m long) for scale; top of handle is at top of weakly organic A horizon paleosol. See plate 1 for sample location and table B1 for specific information and results of radiocarbon analysis.

APPENDIX C

SCARP PROFILES

We used data from topographic profiles across fault scarps, measured perpendicular to the strike of the fault, to evaluate the timing and amount of vertical offset of scarp-forming earthquakes on the Levan and Fayette segments. During reconnaissance mapping in 1984, Machette measured 25 profiles on the Levan segment and 15 profiles on the Fayette segment using a telescoping stadia rod and Abney level. In 2004, Hylland and C.B. DuRoss (Utah Geological Survey) measured 12 additional scarp profiles (six on each segment); we used a telescoping stadia rod and Abney level for the profiles on the Levan segment, and a laser range finder loaned to us by R.L. Bruhn (University of Utah) for the profiles on the Fayette segment. Figure C1 shows general locations of the profiles, and tables C1 and C3 give location data.

The field measurements were reduced to horizontal and vertical coordinates using spreadsheet software, and the resulting plots were manipulated using graphics software to produce profiles having no vertical exaggeration. We used these profiles to determine scarp heights, slope angles, and geomorphic surface offsets; tables C2 and C4 summarize the profile data, and figures C2 and C3 show the unannotated profiles. A few of the profiles measured in 1984 could not be used to obtain needed analysis parameters, so new profiles were measured in 2004 in similar locations as the original profiles. To determine the timing of scarp formation, the data were evaluated using the empirical method of Bucknam and Anderson (1979), which considers scarp height and maximum scarp-slope angle, and the nonlinear diffusion model of Andrews and Bucknam (1987), which calculates a scarp age using surface offset and mass diffusivity (i.e., erosion rate). Hylland (2007b) discussed details of the profile data, analyses, and interpretation.

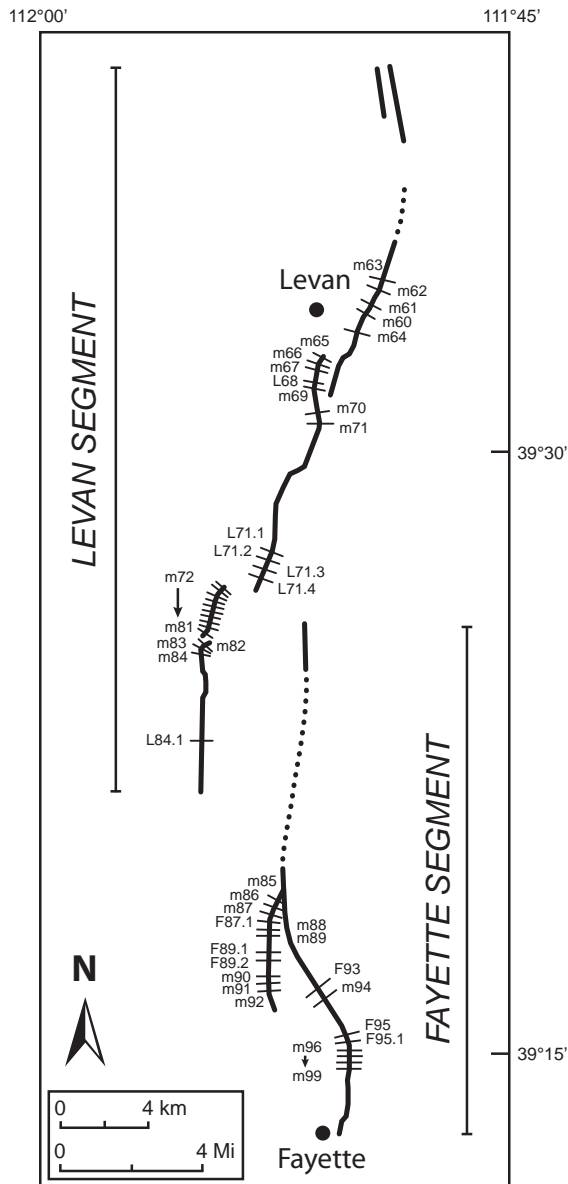


Figure C1. Simplified fault-trace map of the Levan and Fayette segments, showing approximate scarp-profile locations. Location data summarized in tables C1 and C3, profile data summarized in tables C2 and C4, and profiles shown on figures C2 and C3.

Scarp Profiles on the Levan Segment

Table C1. Location data for scarp profiles on the Levan segment.

| Profile ¹ | Measured by ² | Date | UTM (zone 12) coordinates ³ (m) | | North American datum |
|----------------------|--------------------------|---------|--|----------|----------------------|
| | | | Easting | Northing | |
| m63 | MNM | 6/8/84 | 04 28800 | 43 79970 | 1927 |
| m62 | MNM | 6/8/84 | 04 28730 | 43 79820 | 1927 |
| m61 | MNM | 6/8/84 | 04 28650 | 43 79420 | 1927 |
| m60 | MNM | 6/8/84 | 04 28650 | 43 79360 | 1927 |
| m64 | MNM | 6/8/84 | 04 27420 | 43 77100 | 1927 |
| m65 | MNM | 6/8/84 | 04 25850 | 43 74950 | 1927 |
| m66 | MNM | 6/8/84 | 04 25830 | 43 74790 | 1927 |
| m67 | MNM | 6/8/84 | 04 25840 | 43 74720 | 1927 |
| L68 | MDH/CBD | 9/16/04 | 04 25767 | 43 74542 | 1983 |
| m69 | MNM | 6/8/84 | 04 25800 | 43 74430 | 1927 |
| m70 | MNM | 6/8/84 | 04 25890 | 43 73720 | 1927 |
| m71 | MNM | 6/9/84 | 04 25990 | 43 73310 | 1927 |
| L71.1 | MDH/CBD | 9/16/04 | 04 23818 | 43 67944 | 1983 |
| L71.2 | MDH/CBD | 9/16/04 | 04 23208 | 43 66909 | 1983 |
| L71.3 | MDH/CBD | 9/16/04 | 04 23141 | 43 66708 | 1983 |
| L71.4 | MDH/CBD | 9/16/04 | 04 23116 | 43 66375 | 1983 |
| m72 | MNM | 6/13/84 | 04 21430 | 43 65100 | 1927 |
| m73 | MNM | 6/13/84 | 04 21370 | 43 64910 | 1927 |
| m74 | MNM | 6/13/84 | 04 21390 | 43 64860 | 1927 |
| m75 | MNM | 6/13/84 | 04 21380 | 43 64830 | 1927 |
| m76 | MNM | 6/13/84 | 04 21340 | 43 64580 | 1927 |
| m77 | MNM | 6/13/84 | 04 21310 | 43 64430 | 1927 |
| m78 | MNM | 6/13/84 | 04 21230 | 43 64250 | 1927 |
| m79 | MNM | 6/13/84 | 04 21210 | 43 64120 | 1927 |
| m80 | MNM | 6/13/84 | 04 21210 | 43 64080 | 1927 |
| m81 | MNM | 6/13/84 | 04 21260 | 43 63920 | 1927 |
| m82 | MNM | 6/13/84 | 04 21050 | 43 63730 | 1927 |
| m83 | MNM | 6/13/84 | 04 20930 | 43 63660 | 1927 |
| m84 | MNM | 6/13/84 | 04 20850 | 43 63580 | 1927 |
| L84.1 | MDH/CBD | 9/16/04 | 04 20803 | 43 59090 | 1983 |

¹Listed north to south.²CBD, C.B. DuRoss (UGS); MDH, M.D. Hylland (UGS); MNM, M.N. Machette (USGS).³Approximate Universal Transverse Mercator coordinates at middle of profile. UTM coordinates for profiles designated "m" digitized from unpublished (1984) reconnaissance maps by Machette; rounded to nearest 10 m. Coordinates for profiles designated "L" from handheld-GPS field measurements; rounded to nearest 1 m.

Table C2. Scarp-profile data for the Levan segment.

| Profile | H _s (m) | H _m (m) | S (m) | S _{net} (m) | θ (°) | θ' (°) | γ (°) | Comments |
|---------|--------------------|--------------------|-------|----------------------|-------|--------|-------|---|
| m63 | 2.5 | – | 2.0 | 1.2 | 24 | – | 5 | SES; near north end of Holocene trace |
| m62 | 2.5 | – | 1.7 | 1.4 | 27 | – | 8 | SES |
| m61 | 3.8 | – | – | – | 30 | – | 10 | SES; deposition on hanging wall precludes S measurement; min. H |
| m60 | 3.1 | – | 2.2 | 1.5 | 30 | – | 8 | SES |
| m64 | – | 12.2 | 8.1 | 4.8 | 27 | 12 | 5 | MES; rounded crest |
| m65 | 3.2 | – | 2.5 | 1.8 | 28 | – | 7 | SES |
| m66 | 3.0 | – | 2.2 | 1.9 | 28 | – | 7 | SES |
| m67 | 4.3 | – | 2.7 | 2.0 | 32 | – | 12 | SES |
| L68(u) | 2.9 | – | – | – | 26 | – | 7 | SES; upper of scarp doublet; unable to measure S |
| L68(l) | 0.7 | – | – | – | 10 | – | 7 | SES; lower of scarp doublet; unable to measure S |
| m69 | 0.9 | – | 0.5 | 0.5 | 17 | – | 8 | SES |
| m70 | 2.7 | – | 2.0 | 2.0 | 22 | – | 5 | SES |
| m71 | 3.2 | – | 2.3 | 2.0 | 25 | – | 4 | SES; Deep Creek fault exposure |
| L71.1 | 1.7 | – | 1.5 | 1.5 | 10 | – | 1 | SES; θ likely diminished by livestock |
| L71.2 | 1.7 | – | 1.4 | 1.4 | 19 | – | 4 | SES |
| L71.3 | 2.6 | – | 1.9 | 1.9 | 21 | – | 7 | SES |
| L71.4 | 1.4 | – | 1.2 | 1.2 | 22 | – | 2 | SES |
| m72 | – | 2.7 | 2.0 | 2.0 | 18 | 10 | 5 | MES; bevel |
| m73 | – | 1.7 | 1.2 | 1.2 | 15 | 7 | 4 | MES; bevel |
| m74 | – | 1.2 | 0.7 | 0.7 | 11 | – | 5 | MES(?); simple morphology; small H |
| m75 | – | 2.1 | 1.7 | 1.7 | 16 | 7 | 4 | MES; bevel |
| m76 | – | 2.6 | 1.9 | 1.9 | 19 | – | 4 | MES; simple morphology |
| m77 | – | 3.9 | 3.1 | 3.1 | 22 | 7 | 3 | MES; bevel |
| m78 | – | 3.6 | 2.7 | 2.7 | 25 | – | 6 | MES; simple morphology; north of Skinner Peaks trench site |
| m79 | – | 3.6 | 3.1 | 3.1 | 25 | – | 4 | MES; simple morphology; rounded crest; south of Skinner Peaks trench site |
| m80 | – | 1.6 | 1.3 | 1.3 | 17 | – | 3 | MES(?); simple morphology; small H |
| m81 | – | 2.2 | 1.8 | 1.8 | 18 | 10 | 3 | MES; bevel; end of trace at left step |
| m82 | – | 3.1 | 2.7 | 2.7 | 20 | – | 3 | MES(?); simple morphology; end of trace at left step |
| m83 | – | 3.9 | 3.0 | 3.0 | 25 | 21 | 5 | MES; slight bevel |
| m84 | – | 3.8 | 2.6 | 2.6 | 22 | – | 7 | MES; simple morphology |
| L84.1 | – | 2.0 | 1.9 | 1.9 | 15 | 6 | 1 | MES; bevel; near south end of segment |

Profiles are listed north-to-south; see figure C1 and table C1 for location information.

Measurement error is $\pm 10\%$ for scarp height and surface offset, and $\pm 2^\circ$ for scarp- and surface-slope angles.

Symbols and abbreviations:

H_s, scarp height (single-event)

H_m, scarp height (multiple-event)

S, surface offset (at scarp)

S_{net}, net surface offset across zone of deformation

θ, maximum scarp-slope angle

θ', secondary scarp-slope angle

γ, surface- (far-field) slope angle

MES, multiple-event scarp

SES, single-event scarp

l, lower scarp

u, upper scarp

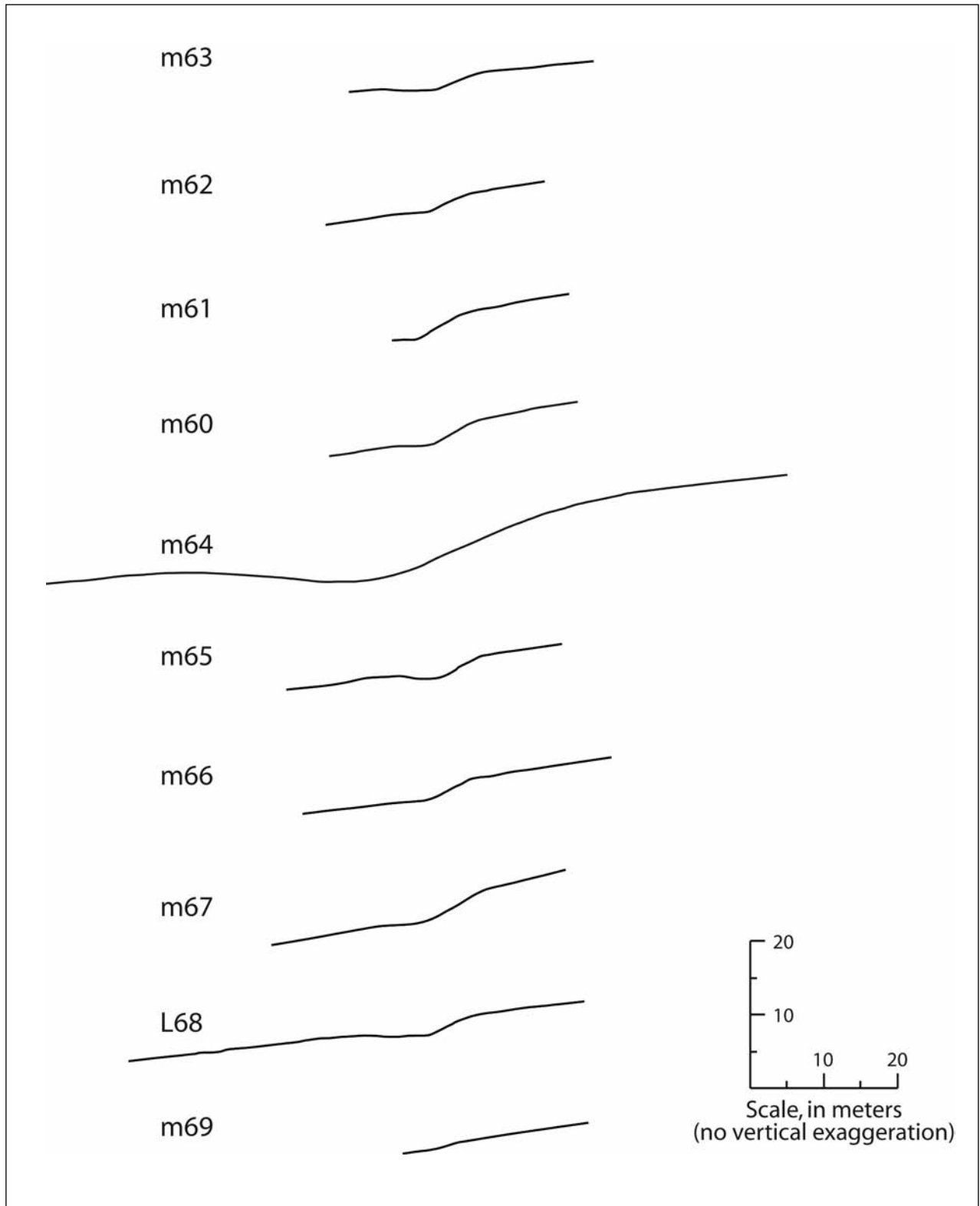


Figure C2. Levan-segment scarp profiles. Profiles arranged from north (top) to south (bottom); see figure C1 and table C1 for location information. Profile data summarized in table C2.

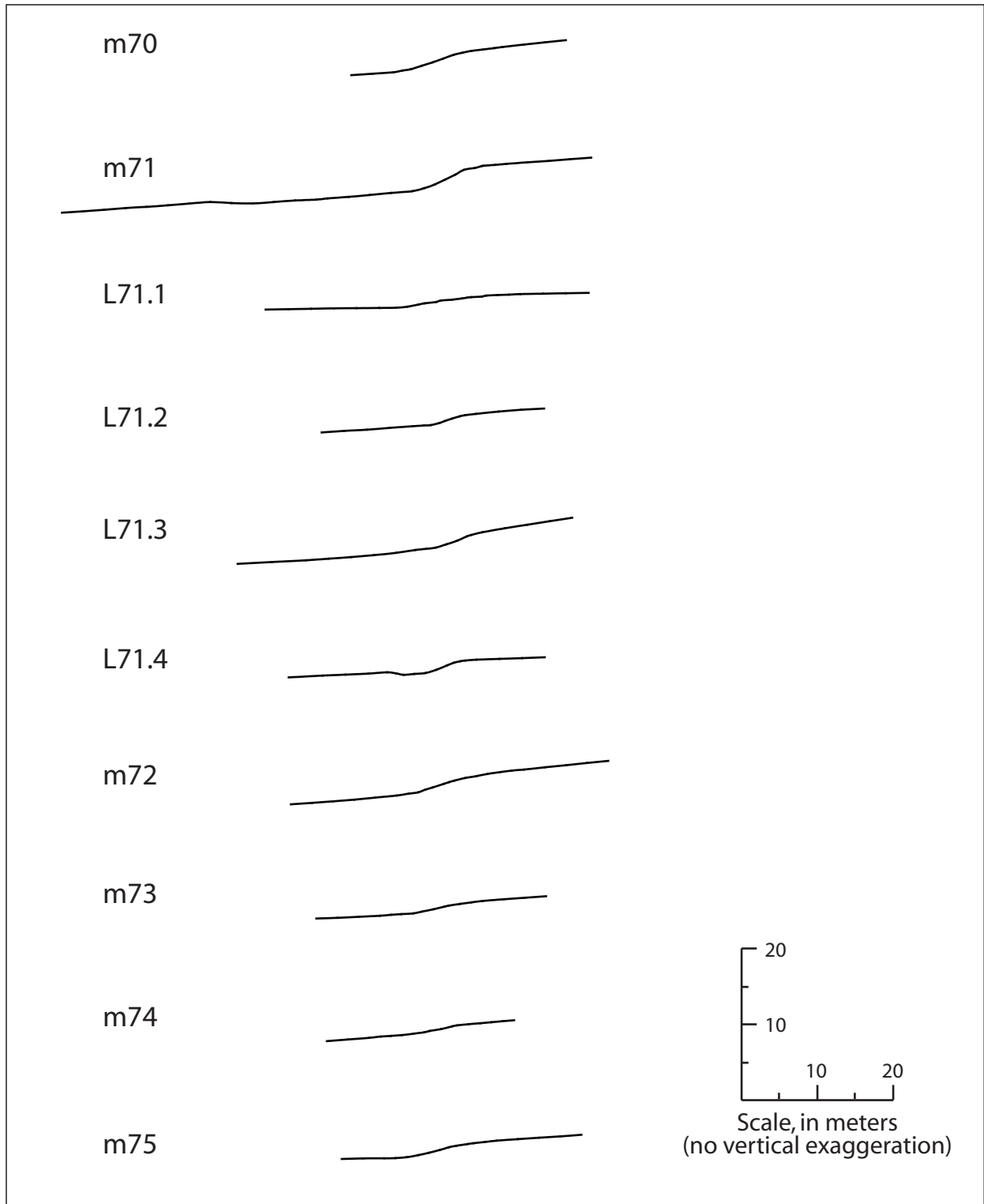


Figure C2 (continued).

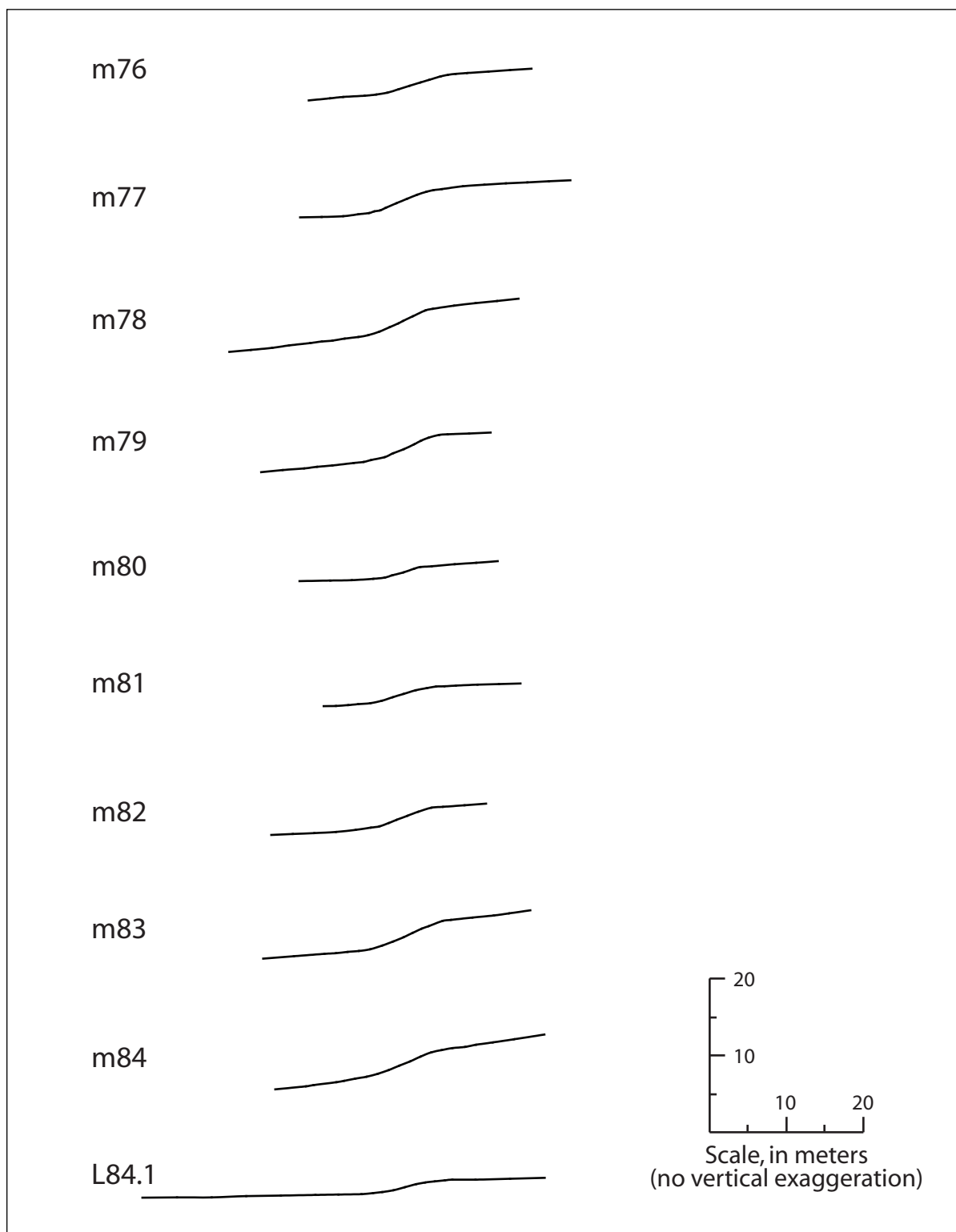


Figure C2 (continued).

Scarp Profiles on the Fayette Segment

Table C3. Location data for scarp profiles on the Fayette segment.

| Profile ¹ | Measured by ² | Date | UTM (zone 12) coordinates ³ (m) | | North American datum |
|-----------------------------|--------------------------|---------|--|----------|----------------------|
| | | | Easting | Northing | |
| Southwestern strand: | | | | | |
| m85 | MNM | 6/21/84 | 04 28730 | 43 79820 | 1927 |
| m86 | MNM | 6/21/84 | 04 28650 | 43 79420 | 1927 |
| m87 | MNM | 6/21/84 | 04 28650 | 43 79360 | 1927 |
| F87.1 | MDH/CBD | 9/17/04 | 04 27420 | 43 77100 | 1983 |
| m88 | MNM | 6/21/84 | 04 25850 | 43 74950 | 1927 |
| m89 | MNM | 6/21/84 | 04 25830 | 43 74790 | 1927 |
| F89.1 | MDH/CBD | 9/17/04 | 04 25840 | 43 74720 | 1983 |
| F89.2 | MDH/CBD | 9/17/04 | 04 25767 | 43 74542 | 1983 |
| m90 | MNM | 6/21/84 | 04 25800 | 43 74430 | 1927 |
| m91 | MNM | 6/21/84 | 04 25890 | 43 73720 | 1927 |
| m92 | MNM | 6/21/84 | 04 25990 | 43 73310 | 1927 |
| Southeastern strand: | | | | | |
| F93 | MDH/CBD | 9/17/04 | 04 23818 | 43 67944 | 1983 |
| m94 | MNM | 6/21/84 | 04 23208 | 43 66909 | 1927 |
| F95 | MDH/CBD | 9/17/04 | 04 23141 | 43 66708 | 1983 |
| F95.1 | MDH/CBD | 9/17/04 | 04 23116 | 43 66375 | 1983 |
| m96 | MNM | 6/22/64 | 04 21430 | 43 65100 | 1927 |
| m97 | MNM | 6/22/64 | 04 21370 | 43 64910 | 1927 |
| m98 | MNM | 6/22/64 | 04 21390 | 43 64860 | 1927 |
| m99 | MNM | 6/22/64 | 04 21380 | 43 64830 | 1927 |

¹Listed north to south.

²CBD, C.B. DuRoss (UGS); MDH, M.D. Hylland (UGS); MNM, M.N. Machette (USGS).

³Approximate Universal Transverse Mercator coordinates at middle of profile. UTM coordinates for profiles designated "m" digitized from unpublished reconnaissance maps (1984) by Machette; rounded to nearest 10 m. Coordinates for profiles designated "F" from handheld-GPS field measurements; rounded to nearest 1 m.

Table C4. Scarp-profile data for the Fayette segment.

| Profile | H _s (m) | H _m (m) | S (m) | S _{net} (m) | θ (°) | θ' (°) | γ (°) | Comments |
|-----------------------------|--------------------|--------------------|-------|----------------------|-------|--------|-------|---|
| Southwestern strand: | | | | | | | | |
| m85 | – | 18.5 | 11.0 | 11.0 | 21 | 17 | 8 | MES; rounded crest |
| m86 | 2.1 | – | 0.9 | 0.9 | 16 | – | 8 | SES |
| m87 | 2.6 | – | 1.6 | 1.6 | 24 | (17) | 8 | SES(?); apparent bevel |
| F87.1 | – | 19.5 | 14.0 | 14.0 | 22 | – | 5 | MES; max. θ at base; upper scarp rounded; deposition on hanging wall, min. H and S |
| m88(u) | 0.8 | – | 0.4 | 0.4 | 15 | – | 7 | SES; upper of scarp doublet |
| m88(l) | 1.1 | – | 0.6 | 0.6 | 17 | – | 7 | SES; lower of scarp doublet |
| m89 | – | 22.5 | – | – | 27 | 21 | – | MES; max. θ at base; upper scarp rounded; deposition on hanging wall, min. H; footwall erosion precludes estimating S |
| F89.1 | 2.0 | – | 1.6 | 1.6 | 7 | – | 2 | SES; θ likely diminished by livestock |
| F89.2 | 1.5 | – | 1.0 | 1.0 | 8 | – | 3 | SES; θ likely diminished by livestock |
| m90 | 1.9 | – | 1.2 | 0.8 | 25 | (13) | 9 | SES(?); apparent bevel |
| m91 | 2.3 | – | 1.4 | 1.3 | 20 | (9) | 5 | SES(?); apparent bevel |
| m92 | 1.8 | – | 1.4 | 1.1 | 17 | (7) | 3 | SES(?); apparent bevel |
| Southeastern strand: | | | | | | | | |
| F93 | – | 4.9 | 2.8 | 2.8 | 14 | 10 | 5 | MES: slight bevel |
| m94 | – | 4.3 | 2.7 | 2.7 | 16 | 8 | 4 | MES: bevel |
| F95 | 2.9 | – | 1.7 | 1.3 | 15 | (10) | 5 | SES(?); apparent bevel |
| F95.1 | 1.8 | – | 1.1 | 1.1 | 10 | – | 5 | SES |
| m96 | 1.3 | – | 1.0 | 0.8 | 10 | (6) | 2 | SES(?); apparent bevel |
| m97 | 1.3 | – | 1.0 | 0.5 | 7 | – | 2 | SES |
| m98 | 1.2 | – | 0.9 | 0.9 | 14 | – | 2 | SES |
| m99 | – | 5.6 | 3.2 | 3.2 | 18 | 15 | 7 | MES; rounded crest; deposition on hanging wall, min. H and S |

Profiles are listed north-to-south; see figure C1 and table C3 for location information.

Measurement error is ±10% for scarp height and surface offset, and ±2° for scarp- and surface-slope angles.

Symbols and abbreviations:

- H_s, scarp height (single-event)
- H_m, scarp height (multiple-event)
- S, surface offset (at scarp)
- S_{net}, net surface offset across zone of deformation
- θ, maximum scarp-slope angle
- θ', secondary scarp-slope angle
- γ, surface- (far-field) slope angle
- MES, multiple-event scarp
- SES, single-event scarp
- l, lower scarp
- u, upper scarp

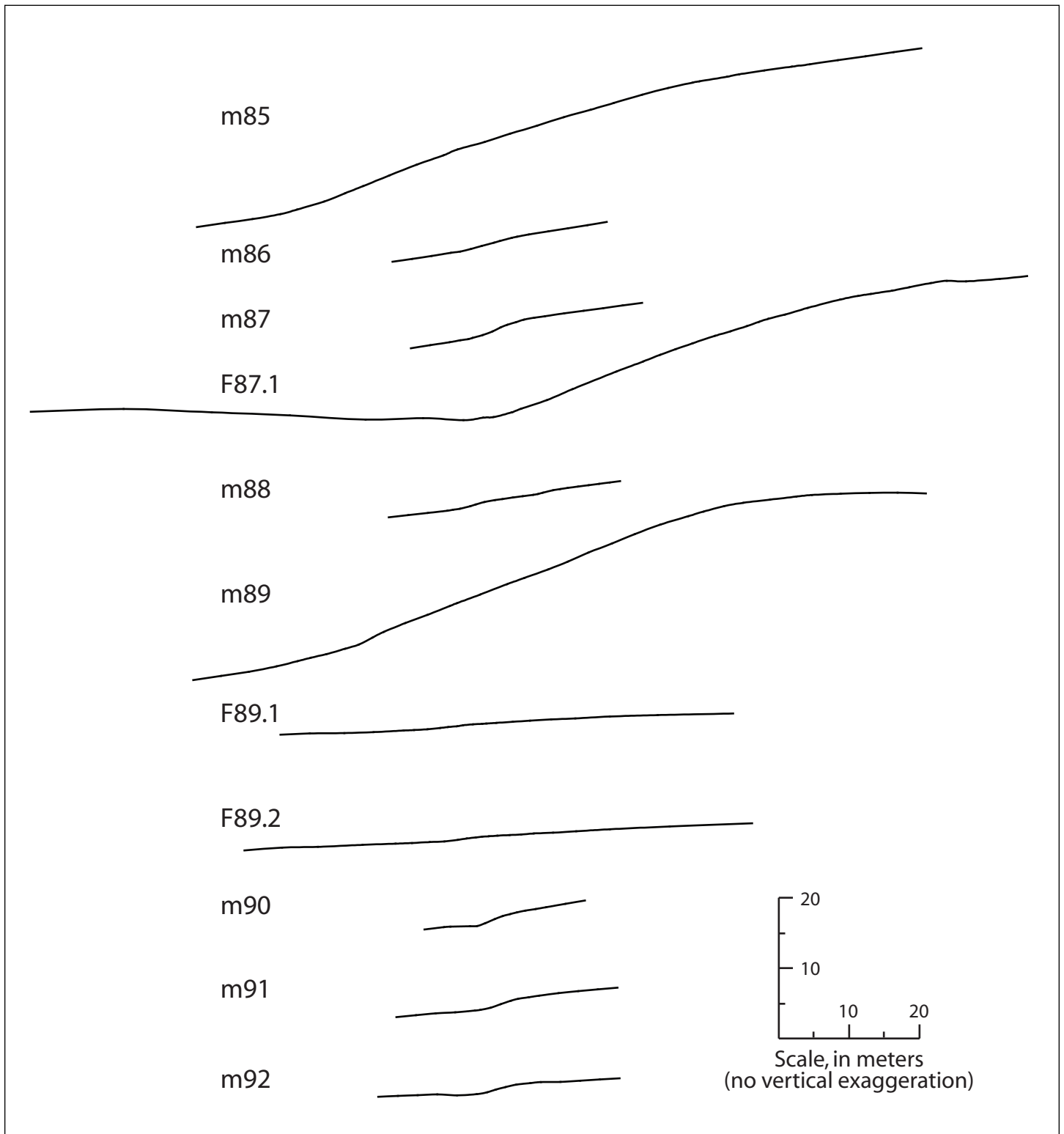


Figure C3. Fayette-segment scarp profiles (SW strand). Profiles arranged from north (top) to south (bottom); see figure C1 and table C3 for location information. Profile data summarized in table C4.

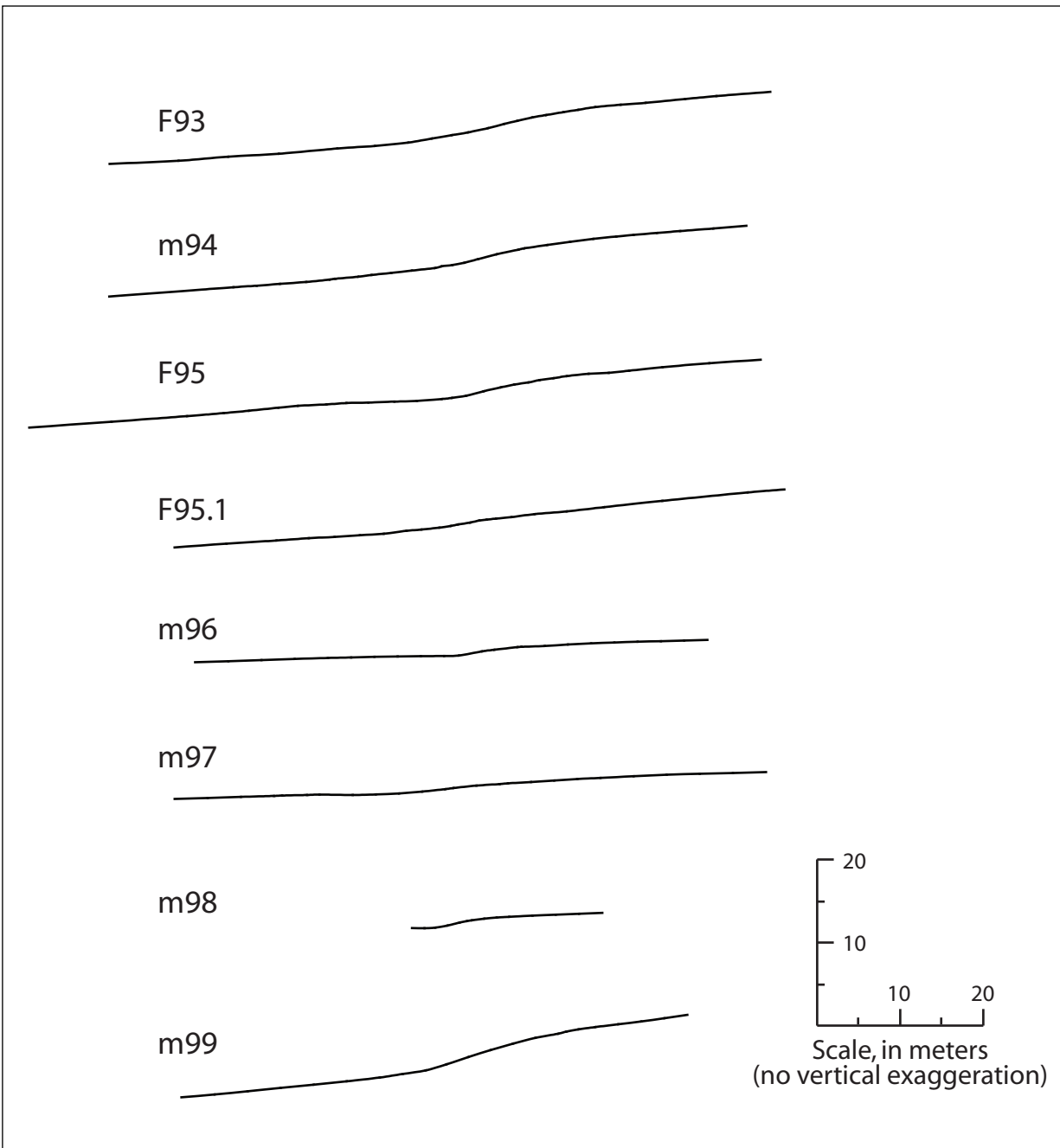


Figure C3 (continued). Fayette-segment scarp profiles (SE strand).